SAND REPORT

SAND2003-0302
Unlimited Release
Printed January 2003

Accident Conditions versus Regulatory Tests for NRC-Approved UF_6 Packages

G. Scott Mills, Douglas J. Ammerman and Carlos Lopez

Prepared by
Sandia National Laboratories
Albuquerque, New Mexico 87185 and Livermore, California 94550

Sandia is a multiprogram laboratory operated by Sandia Corporation,
a Lockheed Martin Company, for the United States Department of Energy's
National Nuclear Security Administration under Contract DE-AC04-94-AL85000.

Issued by Sandia National Laboratories, operated for the United States Department of Energy by Sandia Corporation.

Available to DOE and DOE contractors from
U.S. Department of Energy
Office of Scientific and Technical Information
P.O. Box 62
Oak Ridge, TN 37831

Telephone: (865)576-8401
Facsimile: (865)576-5728
E-Mail: reports@adonis.osti.gov
Online ordering: http://www.doe.gov/bridge

Available to the public from
U.S. Department of Commerce
National Technical Information Service
5285 Port Royal Rd
Springfield, VA 22161

Telephone: (800)553-6847
Facsimile: (703)605-6900
E-Mail: orders@ntis.fedworld.gov
Online order: http://www.ntis.gov/help/ordermethods.asp?loc=7-4-0#online

SAND2003-0302
Unlimited Release
Printed January 2003

Accident Conditions versus Regulatory Tests for NRC-Approved UF_6 Packages

G. Scott Mills, Douglas J. Ammerman and Carlos Lopez
Transportation Risk and Packaging Department
Sandia National Laboratories
P.O. Box 5800
Albuquerque, NM 87185-0718

Work was funded by U.S. NRC Contract J5391

ABSTRACT

The Nuclear Regulatory Commission (NRC) approves new package designs for shipping fissile quantities of UF_6. Currently there are three packages approved by the NRC for domestic shipments of fissile quantities of UF_6: NCI-21PF-1; UX-30; and ESP30X. For approval by the NRC, packages must be subjected to a sequence of physical tests to simulate transportation accident conditions as described in 10 CFR Part 71. The primary objective of this project was to relate the conditions experienced by these packages in the tests described in 10 CFR Part 71 to conditions potentially encountered in actual accidents and to estimate the probabilities of such accidents.

Comparison of the effects of actual accident conditions to 10 CFR Part 71 tests was achieved by means of computer modeling of structural effects on the packages due to impacts with actual surfaces, and thermal effects resulting from test and other fire scenarios. In addition, the likelihood of encountering bodies of water or sufficient rainfall to cause complete or partial immersion during transport over representative truck routes was assessed. Modeled effects, and their associated probabilities, were combined with existing event-tree data, plus accident rates and other characteristics gathered from representative routes, to derive generalized probabilities of encountering accident conditions comparable to the 10 CFR Part 71 conditions.

This analysis suggests that the regulatory conditions are unlikely to be exceeded in real accidents, i.e. the likelihood of UF_6 being dispersed as a result of accident impact or fire is small. Moreover, given that an accident has occurred, exposure to water by fire-fighting, heavy rain or submersion in a body of water is even less probable by factors ranging from 0.5 to 8E-6.

CONTENTS

FIGURES

TABLES

1.0 INTRODUCTION

The Nuclear Regulatory Commission (NRC) approves new package designs for shipping fissile quantities of UF_6. Currently there are three packages approved by the NRC for domestic shipments of fissile quantities of UF_6: NCI-21PF-1; UX-30; and ESP30X.

Packages approved by the NRC have been subjected to a sequence of physical tests to simulate transport accident conditions as described in 10 CFR Part 71 [1.1]. The physical tests consist of a 30-foot drop onto an unyielding surface, a 40-inch drop onto a puncture bar, a 30-minute fully engulfing fire, and water immersion. These designs must demonstrate that there has been no water infiltration into nor any loss of radioactive contents from the package following the tests described in 10 CFR Part 71. NRC approval of these UF_6 packages has been largely based on the packages' tested ability to withstand the hypothetical accident conditions of 10 CFR Part 71.

The objective of the project described in this report was to evaluate the performance of the three NRC-approved UF_6 packages and, in particular, relate the conditions experienced by these packages in the tests described in 10 CFR Part 71 to conditions potentially encountered in actual accidents.

1.1 Summary Of Prior Work

SNL has carried out numerous studies of package performance for spent-fuel casks and other Type B packages, the most recent of which is NUREG/CR-6672 [1.2], a reexamination of truck and rail spent-fuel transportation risks. Furthermore, SNL has performed a wide array of physical tests, and structural and thermal analyses, on Type B packages and their vehicular carriers under various severe accident conditions up to and including extra-regulatory environments; analyses of spent nuclear fuel packages were carried out most recently for preparation of NUREG/CR-6672.

As a part of the effort on NUREG/CR-6672, new accident statistics were developed for truck and rail transportation in the United States and event trees originally developed in NUREG/CR-4829 [1.3] were updated. The appropriate portions of his work were immediately applicable to the present truck-transportation study because the general transportation modal environments for UF_6 and spent-fuel packages are identical.

Differences from NUREG/CR-6672 associated with differences in potential routes used for UF_6 transportation were addressed through use of the Sandia geographical information system (GIS) for transportation and methods for rapidly assessing the properties of any overland route in the United States. These properties included roadside hardness, surface-water crossings, population densities, etc. on a very high-resolution scale (1 kilometer or less, depending on the particular property). Population data were based on the 2000 Census at the highest publicly-available resolution, i.e. Census blocks.

Differences in package construction and materials between UF_6 packages and spent-fuel casks could result in somewhat different responses of UF_6 packages to given accident environments. This study does consider the differences in response between spent-fuel packages and UF_6 packages.

1.2 Assessment Of Technical Issues

SNL experts in package testing and analysis reviewed information regarding the three UF_6 packages (NCI-21PF-1, UX-30, and ESP-30X) currently approved for domestic shipment of fissile quantities of UF_6. Primary information was obtained from NRC-furnished copies of the Safety Analysis Report, Safety Evaluation Report, and Certificate of Compliance for each of the three packages. Regulatory requirements of 10 CFR Part 71 were also reviewed and an initial list of accident scenarios for comparison with these regulatory requirements was developed.

The three UF_6 package designs were examined to determine whether they are sufficiently similar that a single model could be analyzed, e.g. the extent to which structural materials and structures are similar for the three packages was determined. This assessment greatly reduced the number of parameter values that had to be considered in a model of UF_6 package responses to impact forces, for example. Being less time-consuming and more cost-effective than modeling all three packages, this approach permitted completion of this project in the allotted time and budget.

Typical transportation configurations, routes, and practices (crew reporting requirements, emergency response arrangements, etc.) were examined in order to determine the extent to which these factors contributed to deviations from the probability values predicted by the NUREG/CR-6672 event trees. Modifications required to tailor the NURGE/CR-6672 event trees for use with the three UF_6 packages were applied to obtain final accident-scenario probabilities. One modification, regarding proximity to surface waters, was included to address the likelihood of water infiltration of the UF_6 package; reaction of UF_6 with water may lead to formation and release of highly toxic HF. The latter was addressed by means of the GIS route-assessment tools developed at SNL, and evaluation of the probability of simultaneous submersion and an accident of a severity sufficient to create a leak path in a UF_6 package.

2.0 DESCRIPTION OF UF_6 PACKAGES

The three packages considered in this study were the NCI-21PF-1 [2.1], UX-30 [2.2] and ESP-30X [2.3], all NRC-approved for domestic shipments of fissile quantities of UF_6. Each consists of an overpack, of distinctive design, and a common Model 30B 30-inch UF_6 cylinder which may contain up to 5% enriched, virgin or reprocessed uranium. Each cylinder is limited to 5,020 pounds of UF_6; for reprocessed uranium, the package is further limited to not more than $1{,}150A_2$ (0.0257 Ci) of radioactive materials. The following descriptions are quoted from the respective Safety Analysis Reports.

2.1 Model 30B UF_6 Cylinder

This is the containment vessel in each of the packages; a heavy-walled pressure vessel, it must be fabricated, inspected, tested and maintained in accordance with the latest NRC-approved revisions of USEC-651, and ANSI Standard No. N14.1 [2.4]

2.2 NCI-21PF-1 Protective Shipping Package

The package consists of the 30B cylinder, the overpack (upper and lower half with 10 toggle closures) and a valve protection device (VPD); it is similar to the DOT-21PF-1B overpack. The VPD (3 aluminum inserts, 1 spacer and 1 spider) is designed to prevent two modes of failure: (1) the overpack wall from moving in and impacting the cylinder valve and (2) the cylinder skirt from collapsing into the cylinder valve. Gross weight of the loaded package is 8,870 pounds.

The overpack is constructed of two stainless steel shells:

One outer 43 inch diameter, 92 inch long (14 gage) cylinder with ¼ inch ends

One inner 30-7/8 inch diameter, 82-5/8 inch long (14 gage) cylinder with ¼ inch ends

Annular space filled with fire-retardant, phenolic foam

Disks between end plates filled with oak wood blocks

Overall outside dimensions of the package (including tie-down structures) are 49-1/8 inches by 49-1/8 inches by 92 inches long. There are no inner protrusions and outer protrusions consist of the lifting/tie-down points. A horizontal joint (stepped down to the outside to minimize water in-leakage) between the package halves which are secured by ten 1 inch diameter stainless steel toggles. The tie-down pattern is interchangeable with the DOT-21PF-1A and -1B overpacks.

2.3 UX-30 Protective Shipping Package

The overpack is a right circular cylinder constructed of two stainless steel shells with the volume between the shells filled with 6-inch thick, closed-cell, polyurethane foam (Chem-Nuclear Systems, Inc. Specification No. ES-M-170, Rev. 0). A stepped horizontal joint permits the top half of the overpack to be removed from the base; the two halves are secured with ten indexed, cross-locking “ball lock” pins. The overpack is 43.5 inches in diameter and 96 inches long. The maximum gross weight of the package is 8,270 pounds.

There are no inner protrusions in the UX-30 overpack and the external lifting lugs extend from the overpack on each end or on the sides near the closure interface. The UX-30 is designed to replace the 21PF-1B standard DOT overpack while reducing much of the maintenance required for the 21PF-1B through resistance to moisture of the stainless steel and closed-cell foam.

2.4 ESP-30X Protective Shipping Package

The package is a right circular cylinder constructed of two steel shells, i.e. an outer shell 43 inches ID by 96 inches long and an inner shell 30-7/8 inches ID by 82-5/8 inches long. The volume between the shells, including the space between the ½-inch thick end plates of the two shells, is filled with fire-retardant, closed-cell phenolic foam per ESP Specification ESP-PF-1. There are no inner protrusion of the ESP-30X PSP and outer

protrusions consist of lifting and tie-down points and bolt closures. The tare weight of an empty package is nominally 2,955 pounds; the maximum gross weight of the loaded package is 9,365 pounds. The tie-down bolting pattern is identical with that of the DOT-21PF-1A and -1B overpacks.

A stepped horizontal joint permits the top half of the package to be removed from the base and the horizontal closure joint of each package half is covered with steel. The joint is stepped down to the outside to minimize water in-leakage to the cylinder cavity. The package halves are secured with ten ¾ inch diameter steel bolts and nuts.

3.0 METHODOLOGY

3.1 Event Trees

The event trees developed to support NUREG/CR-6672 [1.2], although developed to evaluate spent-fuel shipments, provided useful and up-to-date accident-related data for evaluation of UF_6 packages transported by overland modes (only truck transport was considered in the present study). Use of data from [1.2] was valid for UF_6 packages because accident frequencies are independent of the nature of the cargo. Furthermore, since water could potentially act as a moderator or generate toxic vapor (HF) if package contents were exposed to it, some event tree branches were modified to characterize the probability of water being present following an accident in which a package might be breached.

To this end, the GIS was used to identify surface waters over which shipments might pass (bridges, overpasses) and beside which they might travel (e.g., lakes, streams within 30 meters of the route). Other potential means of water ingress following an accident of relatively high severity included: inappropriate actions by first responders and severe weather (rain) events. Both of these were accounted for in event-tree extensions using qualitative data on the frequency of inappropriate first-responder actions obtained from the Federal Emergency Management Agency (FEMA), and frequency of heavy rainfall data obtained from a multi-year NOAA database.

3.2 Route Characteristics

Six truck routes, selected by NRC, were characterized using updated, standard tools similar to those employed in NUREG/CR-6672, e.g. route-lengths within regions of rural, suburban, and urban population densities, and population-density-dependent baseline accident rates, were compiled by use of the WebTRAGIS routing code [3.1], the GIS, and heavy-truck accident-rate compilations [3.2].

3.3 Structural Analysis for UF_6 Packages

The NCI-21PF was chosen as a representative package for the structural analysis because the weight of this package is between the weights of the UX-30 and ESP-30X. Also, the construction of all three packages is similar, so use of this package could be expected to give results representative of all of the packages, especially in terms of kinetic energy and force generation. Finite element analyses of the 21PF were performed for impacts at

various angles onto an unyielding target at 30 mph. The kinetic energy time histories from these analyses were used to develop force-displacement curves for the 21PF for each impact angle.

A method has been developed for using a force-displacement curve to relate 30-mph impacts onto an unyielding target to higher-speed impacts onto yielding targets. For each target type considered, a force-deflection relationship for the target was developed. For soil and concrete targets this was done in NUREG-CR/6672. For a relatively soft package, such as the 21PF, impacts with trucks and trains are also of concern. Therefore, force-deflection curves for these objects were developed from existing test data at SNL.

3.4 Thermal Analysis for UF_6 Packages

Even though the three UF_6 overpacks have the same overall dimensions (96 in. long, 43.5 in. diameter, 6 in. thick wall), the UX-30 was selected for this thermal analysis because the thermal conductivity of the polyurethane foam used in the UX-30 is higher and the product of density with specific heat is lower than those of the phenolic foam used in the ESP-30X and the combination of phenolic foam and white oak used in the NCI-21PF-1. Therefore, the internal temperatures of the UX-30 when exposed to hot and transient external conditions will be higher than those for the ESP-30X and the NCI-21PF-1.

Five different accident configurations were modeled in the thermal assessment of the UX-30 packaging.

1) **Fully engulfing**, 10 CFR Part 71 fire,
2) Package offset one meter, **side** facing the fire at ground level,
3) Package offset five meters, **side** facing the fire at ground level,
4) Package offset ten meters, **side** facing the fire at ground level, and
5) Package offset one meter, **end** facing the fire at ground level.

The normal conditions of transport were also modeled in order to compare and validate the model built for this study using the data presented in the Safety Analysis Report (SAR) of the UX-30. The simulation of the 10 CFR Part 71 fire environment provided the data necessary for the comparison of the results obtained from the simulations in which the package was offset from the fire. For the analyses of the package offset from the fire, the fire was modeled as a radiant surface with dimensions representing a fire cross-section.

The gap between the internal surface of the over-pack and the external surface of the UF_6 canister was included in the model as was done in the UX-30 SAR. All modes of heat transfer (i.e., conduction, convection, and radiation) were included in the analyses. In order to establish equivalence of each non-regulatory configuration with the regulatory fire, temperature history plots were generated that determined the time to reach a threshold temperature in the package. The threshold temperature was defined as the maximum temperature of the UF_6 contents at the end of the 30-minute fully engulfing regulatory fire simulation.

4.0 EVENT TREES

The event tree developed in NUREG/CR-6672 [1.2] for truck transport of spent fuel casks is reproduced in Figure 4.1. As employed in that study and in the present study, the event tree describes the basic accident scenarios as they apply to spent fuel casks (and potentially to all Type B packages or equivalents). The probabilities associated with the end-points of the branches must be modified to take account of accident speeds, fire occurrence and, in the present study, exposure to water. These extensions are described more effectively by equations rather than addition of branches to the tree.

Each of the endpoints (except the "Fire only" branch) has an associated probability of occurrence of a fire with sufficient intensity to compromise package containment of the UF_6 directly, or to exacerbate releases resulting from mechanical forces. The probabilities of these events were defined using thresholds determined in the structural and thermal analyses described Sections 6 and 7, and probability distributions developed for NUREG/CR-6672. Mechanical damage thresholds were defined by accident speeds calculated to be equivalent to a 30 mph impact on an unyielding target, as described in the section on structural analysis.

Thermal thresholds were defined by the times required to reach a critical temperature in each of the cases described in the thermal analysis section. For each time, a probability was determined from the appropriate distribution function in NUREG/CR-6672.

For each accident scenario (endpoint in Figure 4.1), a total probability of occurrence was defined by an equation of the form:

P = (event-tree probability)(threshold-speed prob.)(fire prob.)(fire-duration prob.).

As in NUREG/CR-6672, this general form was developed to take into account the fire probabilities relating to different types of collisions:

(fire prob.) = (optically-dense prob.)(flame-temp. prob.)(fire/scenario prob.)

= (0.2)(0.86) (fire/scenario prob.)

for accidents not involving trains and a flame temperature of ~800°C.

= (1.0)(0.86) (fire/scenario prob.)

for train collisions with trucks and a flame temperature of ~800°C.

(Note that the flame-temp. prob. value of 0.86 was interpolated from probabilities of 0.5 for ≥1000°C and 1.0 for >650°C given in Section 7.4.4.3 of NUREG/CR-6672.)

Values of the probability that a fire will occur (fire/scenario prob.) under any of various accident scenarios (Table 7.6 of NUREG/CR-6672) are listed in Table 4.1. In NUREG/CR-6672, an average of the values in Table 4.1 was calculated using the accident scenario probabilities listed in the event tree (Figure 4.1); the resultant average probability that a fire occurs is 0.018. This average value is employed in the calculations of total probability in Section 8.

For the remaining terms in the equation, combinations of event-tree probabilities, speed probabilities for various surfaces, and fire durations for different fire locations were tabulated as shown in the results section.

Certain additional concerns related to the unique character of UF_6 and its interaction with water required additional probabilities to be assessed as described in Sections 4.1 – 4.3 below.

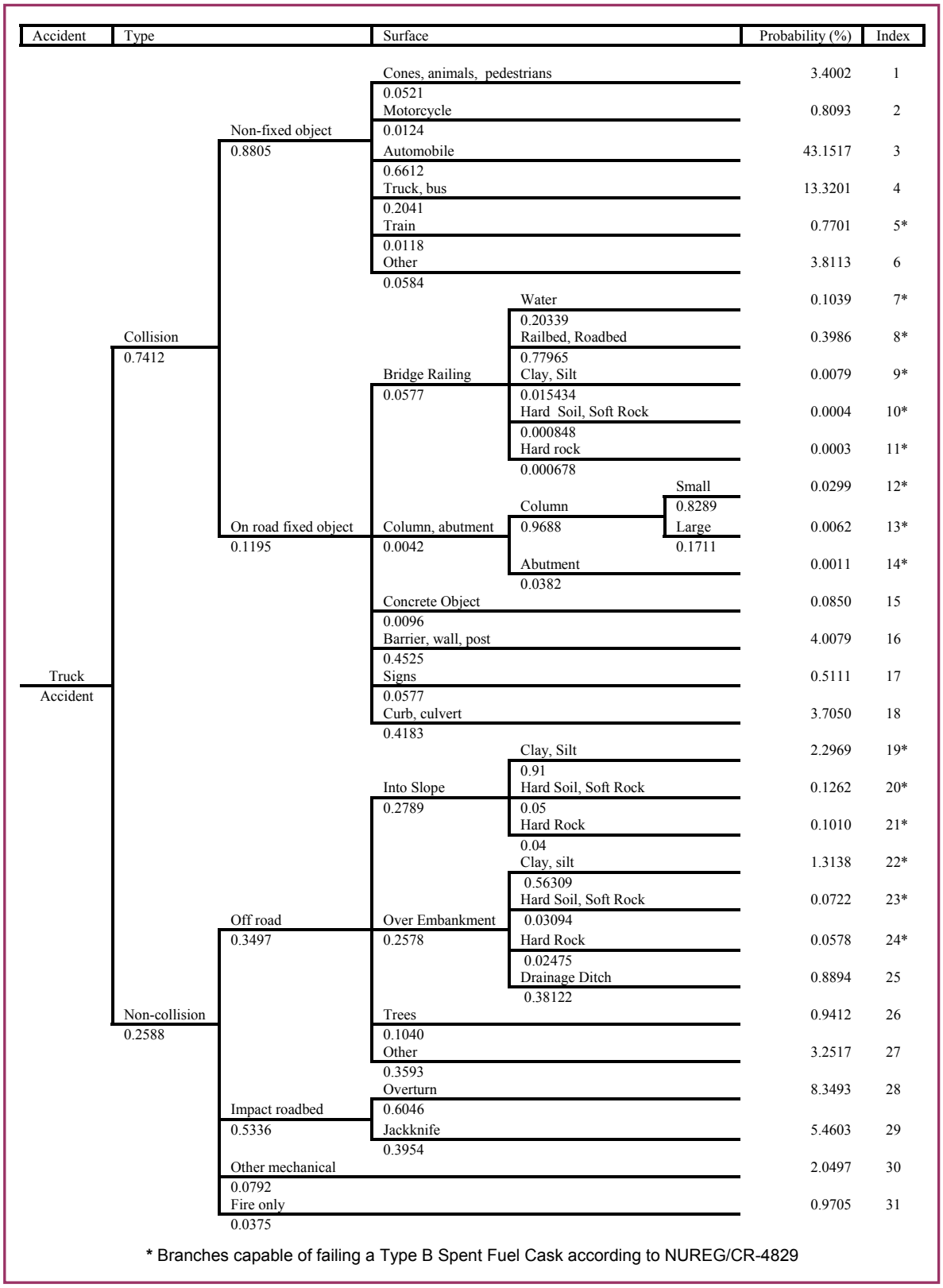

* Branches capable of failing a Type B Spent Fuel Cask according to NUREG/CR-4829

Figure 4.1 – Truck Accident Event Tree from NUREG/CR-6672

Table 4.1 – Truck Accidents that Initiate Fires

	Fraction of Accidents of This Type that Initiate Fires
Collision with	
Car	0.003
Truck	0.008
Other objects	0.013
Non-Collisions	
Ran off road	0.011
Overturns	0.012
Other	0.13

4.1 Actions of First-Responders

The probability of water being applied to a UF_6 package by first-responders was defined by qualitative information from FEMA (private telephone conversation) indicating "if there is a fire, they will put water on it." The same source indicated that quantitative data on these actions are not collected/compiled. The probability that water will be applied by first-responders was estimated to be 50% in the event of a fire (regardless of its size or duration); this is expected to be a conservative estimate.

4.2 Heavy Rainfall Probability

The probability of a significant amount of water being applied by heavy rainfall to a UF_6 package involved in an accident was determined from hourly precipitation amounts (inches), recorded in a NOAA database [4.1], for 39 cities on or near the six routes listed in the next section. As immersion due to rainfall was considered an extremely improbable event, a conservative estimate of achievable rates of rainfall which could lead to intrusion of water into the package contents was calculated. A container lying in the top half of an overpack, with the fill-valve severed, (rolled onto its top with its axis parallel to the road or ground) was hypothesized as the end-state of an accident. Considering the approximate geometry of the container-overpack interface and assuming all rain falling within the outer edges of the overpack would run down into this interface, the possibility for collected water to reach the UF_6 through the severed fill-valve existed after 2 inches of rain, or more, had fallen. If knowledgeable people (not necessarily first-responders) did not reach the scene (and remedy the situation) within one hour, 2 inches of rain per hour would be of concern.

Data for the most recent years available in the NOAA database (1988, 1989 and 1990) were analyzed to identify instances of hourly rainfalls greater than 2 inches; there were eight. Thus, the comprehensive probability of rainwater entering the UF_6 container was calculated from cumulative data from all of the selected routes to be of the order:

$$\frac{8 \text{ (city-hours)}}{(39 \text{ cities})(1096 \text{ days})(24 \text{ hours/day})} \cong 8\text{E-}6 \, .$$

This probability applies to all event tree branches for which sufficient forces are indicated by structural analysis to be capable of severing or seriously damaging the fill-valve. The probability that the entire gap between the UF_6 container and the lower half of the overpack could be filled with water (intrusion through a damaged fill-valve excluded) was considered remote and therefore, "immersion" due to rainfall was considered extremely improbable and was neglected.

4.3 Proximity to Bodies of Water

Overlaying maps of the routes, described in the next section, on maps of U.S. Census blocks by means of the GIS, those blocks which were specified (by database entries describing the individual blocks) as consisting partially or entirely of water were identified. For each route, a total of the route length either crossing or lying within 30 meters of these blocks was calculated. (Note that the actual distance between roadway and water will typically be greater than 30 meters, depending on the size of the census block.) Dividing each total by the full length of the respective route yielded the conservatively high fractions listed in Table 5.1. Typically, portions of a route crossing over rivers, etc. are relatively short and do not contribute significantly to the fractions listed in Table 5.1. The major portion of these fractional values is attributable to route segments bordering rivers and other bodies of water, e.g. Interstate Highway 80 follows the Platte River across a significant portion of Nebraska. Therefore, these fractions were not applied to end-point 7 in Figure 4.1, which represents collision with a bridge guardrail and subsequent fall to water or other surface below. The fractions in Table 5.1 were applied to event-tree branches described as "Off road" on the "Non-collision" branch in Figure 4.1 and are expected to provide a very conservative estimate of the likelihood that a UF_6 shipment could experience immersion in (or intrusion of) water upon departing the highway in an accident.

5.0 ROUTE CHARACTERISTICS

A group of UF_6 shipment origins and destinations was specified by NRC to address domestic shipments of UF_6 between the gaseous diffusion plants (GDPs), and from the GDPs to the US fuel fabricators or to ports of export; import/export shipments of UF_6 were not considered. These origins and destinations are listed in Table 5.1. Representative routes between these points were determined by use of the WebTRAGIS routing code [3.1] which characterizes the routes according to the lengths within Rural, Suburban and Urban population-density zones. In addition, the code calculates a distance-weighted population density for the aggregate of route-segments having population densities within the defined range for each zone: 0 to 66 persons/km^2 is Rural; 67 to 1670 persons/km^2 is Suburban; greater than 1670 persons/km^2 is Urban. These lengths and population densities are also listed for each route in Table 5.1.

The fraction of each route that is either over or within 30 meters of U.S. Census blocks incorporating bodies of water is listed in the fourth column of Table 5.1.

The six routes listed in Table 5.1 are depicted in Figures 5.1 and 5.2. Each route is constrained by the WebTRAGIS routing code to use Interstate Highways unless none is available; the latter condition may occur over short distances at the route origins and/or destinations.

The conditional probabilities described by the event tree in Figure 4.1 assume that an accident has occurred; the probability that an accident, having any of the characteristics identified in the event tree, is defined as the product of the number of accidents per truck-kilometer and the route length. Accident rates, for heavy trucks, have been compiled [3.2] for each of the states from Dept. of Transportation data. Distance-weighted average accident rates for the routes listed in Table 5.1 are listed in the fifth column of the table.

Table 5.1 - Summary of designated-route characteristics

Route	Length[1]	Population Density[2]	Fraction Bordering Or Over Water[3]	Distance-Weighted-Average Accident Rate[4]
Paducah, KY GDP to Portsmouth, OH GDP	R: 559 S: 310 U: 18	R: 21 S: 284 U:2190	0.15	2.8
Portsmouth, OH GDP to Portsmouth, VA	R: 472 S: 348 U: 38	R: 18 S: 345 U:2250	0.12	3.0
Portsmouth, OH GDP to Wilmington, NC	R: 547 S: 409 U: 34	R: 18 S: 360 U:2150	0.07	3.0
Portsmouth, OH GDP to Boston, MA	R: 664 S: 676 U: 117	R: 20 S: 389 U:2590	0.07	4.1
Portsmouth, OH GDP to Hanford, WA	R:3302 S: 695 U: 70	R: 11 S: 303 U:2240	0.15	3.6
Portsmouth, OH GDP to Seattle, WA	R:3340 S: 828 U: 110	R: 12 S: 319 U:2350	0.15	3.6

[1] Length (kilometers) of route within Rural, Suburban and Urban zones.
[2] Distance-weighted-average population densities (persons/km^2) for population residing within ½ mile (0.805 km) of the route centerline.
[3] Fraction of the route over water or within ~30 meters of water as determined from U.S. Census Block data and the GIS.
[4] Average of state accident rates weighted by the length of route in each state traversed (10^7 Veh-km)$^{-1}$

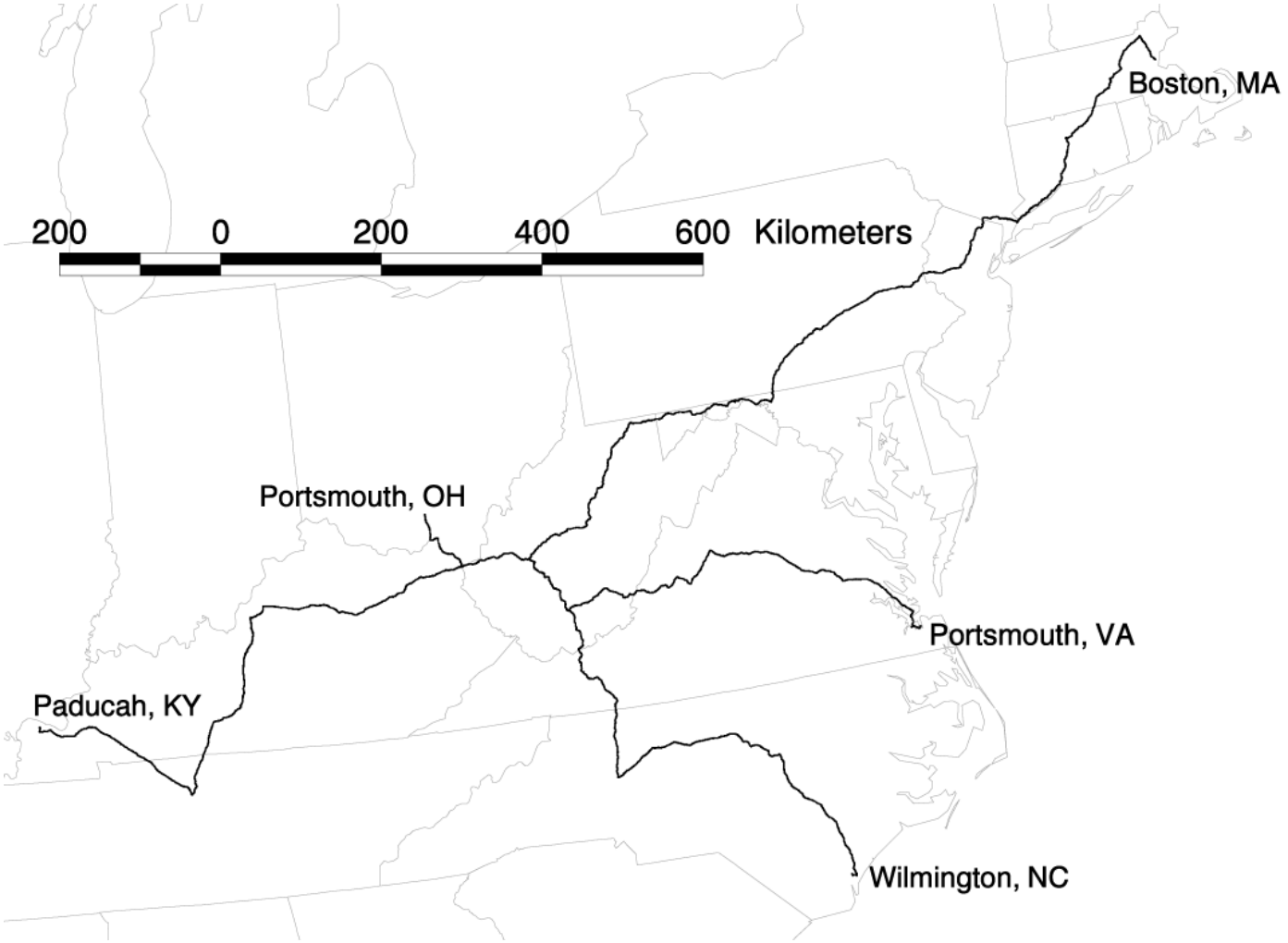

Figure 5.1 – Map of Eastern Routes Employed in the Study

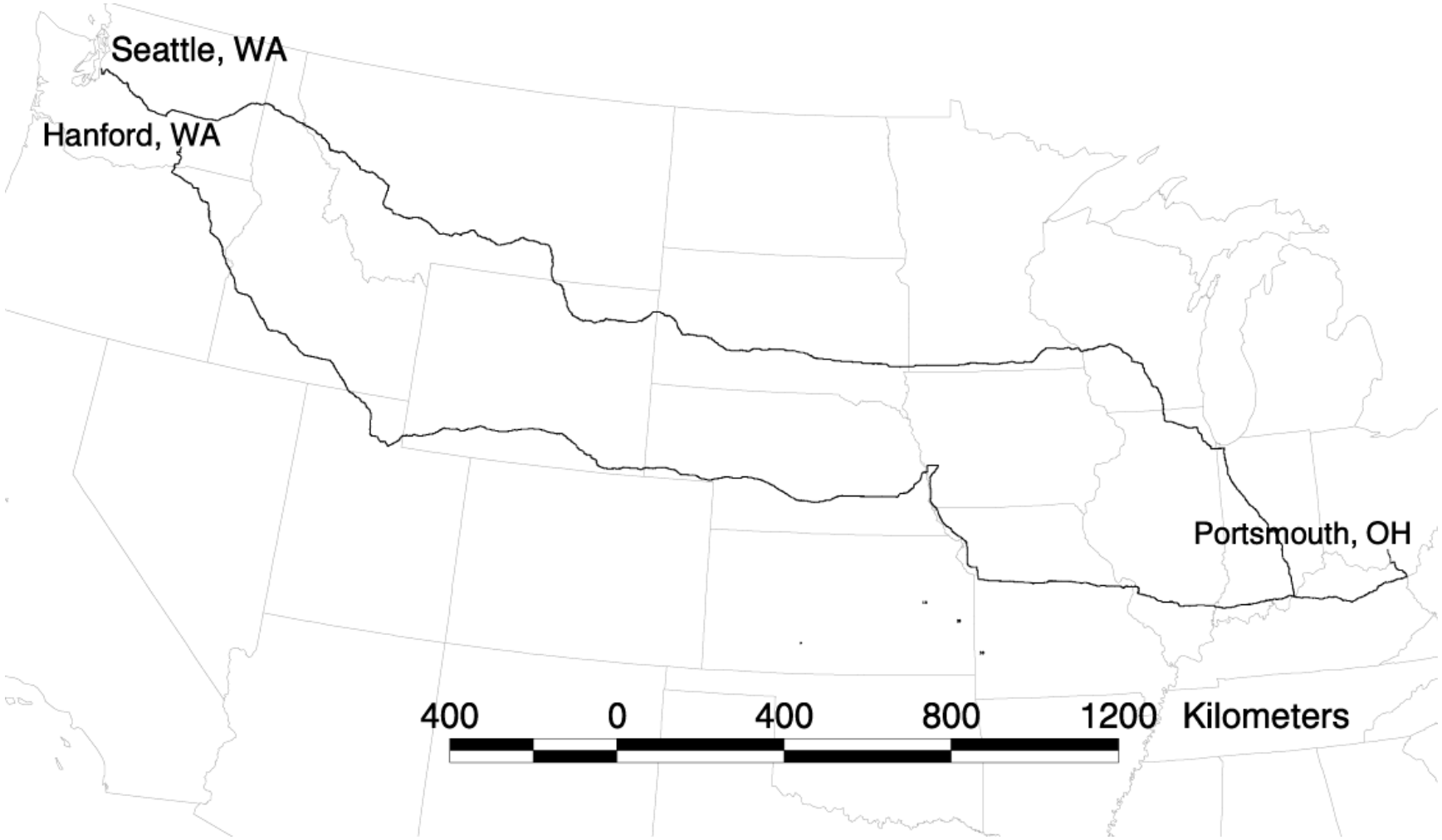

Figure 5.2 – Map of Western Routes Employed in the Study

6.0 STRUCTURAL ANALYSIS - Equivalent Impact Velocities

The packages used to transport UF_6 have been demonstrated to survive (no loss of containment) an impact at 30 mph onto an essentially unyielding target (hypothetical accident conditions of 10 CFR Part 71 [1.1]). In conducting risk assessments, real accidents must be evaluated. Real accidents occur with impacts onto objects that are not unyielding with the consequence that the target absorbs a portion of the impact energy. This fact makes higher speed impacts onto these real targets no more severe than the hypothetical accident impact on an unyielding surface. To determine the velocity for impact onto a real target that has the same severity as the 30 mph impact on an unyielding target, the amount of energy absorbed by the target must be determined [6.1, 6.2]. This section of the report will discuss how that was done for a typical UF_6 transportation package.

6.1 Finite Element Analyses

To compare the response of a typical UF_6 package to an impact onto a yielding target with the regulatory impact onto an unyielding target, the contact force between the package and unyielding target had to be quantified. To do this, finite element analyses of impacts of the NCI-21PF onto an unyielding target, using the Sandia National Laboratories-written explicit dynamic finite element code PRONTO-3D [6.3], were employed. These analyses included impacts at angles of 0° (end impact), 13.5° (CG-over-corner impact), and 75° (slap-down impact). Figure 6.1 shows the finite element mesh used for the analyses. Included in the model are the outer shell of the 21PF, the foam and wood impact absorbing material, the inner shell of the 21PF, the 30B cylinder, and its UF_6 contents. The finite element analysis outputs the total kinetic energy of the package at 100 time steps throughout the simulation time. If it is assumed that all of this kinetic energy is associated with motion in the direction of the impact, then the average velocity of the package at each time can be determined ($KE = ½ mv^2$). The contact force between the package and the unyielding target was calculated by numerically differentiating the velocity to get acceleration and multiplying this by the package mass to get force. A finite element analysis was not performed for impact in the side-on orientation. To approximate a result for this case, the slap-down analysis was used. In the slap-down orientation, only one end of the cask is exerting force at any given time; therefore, it was assumed that the contact force for a side-on impact, where both ends of the cask are exerting force simultaneously, would be twice that for the slap-down case. The displacement of the center-of-gravity (CG) was determined by numerically integrating the velocity. The results of these two operations are plotted together as a force vs. deflection curve for the package in the end-on, CG-over corner, and side-on orientations. Figure 6.2 shows these three curves.

The maximum contact force for the end-on orientation is 2,600,000 pounds. The maximum contact force for the corner and side-on orientations is 1,500,000 pounds. That the maximum contact force for the side-on orientation would be less than the maximum contact force for the end-on orientation is unexpected. This is a result of the conservative way in which the side-on case was derived from the slap-down analysis (doubling of the slap-down result).

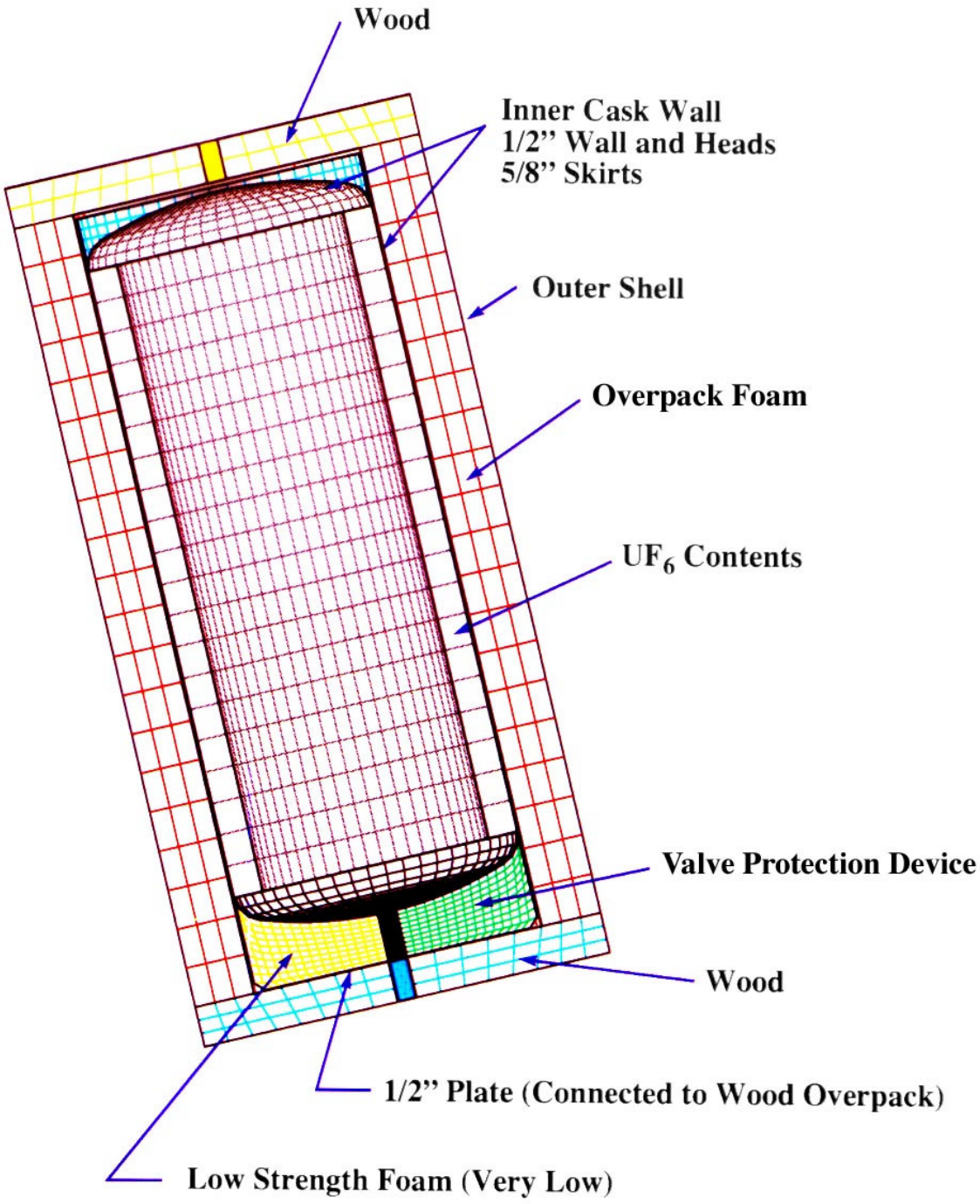

Figure 6.1 - Finite Element Mesh for the NCI-21PF

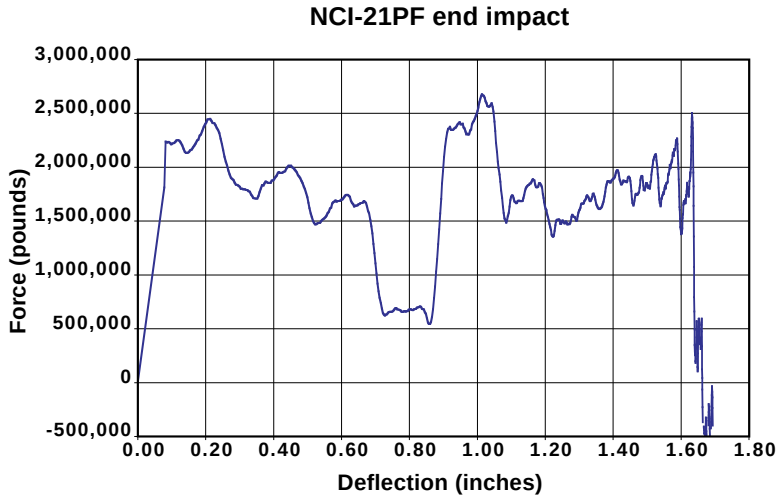

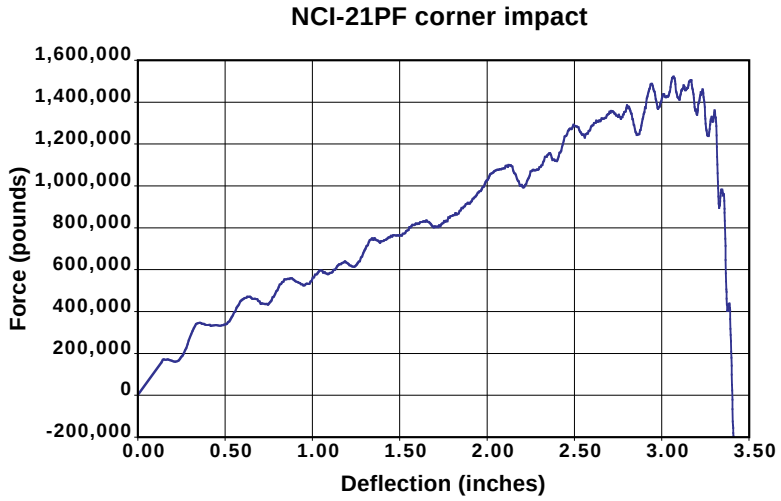

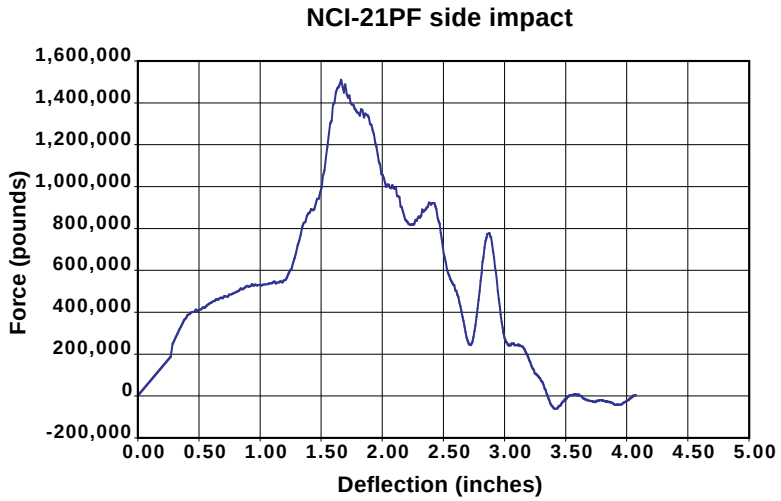

Figure 6.2 - Force-deflection Curves for the NCI-21PF impacting an Unyielding Target

6.2 Impacts on Yielding Targets

In order for an impact on a yielding target to produce as much damage to the cask as the impact on the unyielding target, the contact force between the package and the yielding target has to be as large as the peak contact force between the package and the unyielding target. For the contact force to be of this magnitude, the target must be strong enough to exert this magnitude of force. Impacts with low mass, non-fixed objects, such as automobiles, sign posts, telephone poles, etc. cannot produce a force this large; consequently, none of these impacts is as severe as the regulatory impact, no matter how large the impact velocity. Impacts with objects of large mass, such as trucks and trains, and with fixed surfaces or objects (soil, asphalt, concrete, rock) have the potential to be as severe as the regulatory impact if the impact velocity is sufficiently large.

The general method used to compare impacts with yielding targets to the regulatory impact onto an unyielding target is to calculate the amount of energy absorbed by the target, add this energy to the initial kinetic energy of the package, and compute an equivalent velocity for the package that gives this sum as its kinetic energy. A basic assumption of this method is that the damage to the package as a result of an impact onto a yielding target is in the same mode as the damage due to impact onto the unyielding target. This is generally the case for relatively flat targets or targets for which the impact interface between the package and the target remains essentially planar.

6.2.1 Impacts on Soil Targets

High-speed impacts of radioactive material packages on soils have been studied at Sandia by Gonzales [6.4], Bonzon [6.5], and Waddoups [6.6]. In the work by Gonzales a 20-in diameter steel test article weighing 5200 pounds was impacted onto native desert soil at impact speeds of 30, 45, and 60 MPH in an end-on orientation. These impacts led to penetration distances of 19, 25, and 36 inches, respectively. The tests by Bonzon involved an impact of an LLD-1 plutonium package (2R containment vessel in a outer container) weighing 76 lbs at 460 MPH in a side-on orientation, three impacts of a 10-gallon 6M (2R containment vessel in a 15-inch diameter by 18-inch high drum weighing 55 pounds) (286 MPH in a side-on orientation, 267 MPH in a corner orientation, and 518 MPH in a slapdown orientation), and an impact of a FL-10 package (steel pipe containment vessel in a 110-gal. drum weighing 500 pounds) at 317 MPH in a side-on orientation. The tests by Waddoups involved an impact of a B of E 83 cask weighing 6,720 pounds at 246 MPH and a OD-1 cask weighing 16,300 pounds at 230 MPH. The results of these tests have been used to develop a force-deflection relationship for soil targets being penetrated by a package [6.1]. While the test units used in these tests may be stiffer than a UF_6 package, the stiffness of the package has little impact upon the force generated in the soil for a given penetration distance (the package stiffness only influences the impact velocity required to produce a given penetration), the force is determined by the footprint of the package. Figure 6.3 shows the force-deflection curve for a package with 43-inch diameter impacting in an end-on orientation. The soil impacted in the tests was hard desert soil typical of the region around Albuquerque, NM. To adjust this curve for softer soils, the force was scaled by the number of blows required to produce a one-foot penetration by a cone penetrometer. For hard soils this number is 30, for stiff soils it is 12, for medium soils it is 6, and for soft soils it is 3. The force exerted on the package also depends on the package diameter. For each impact

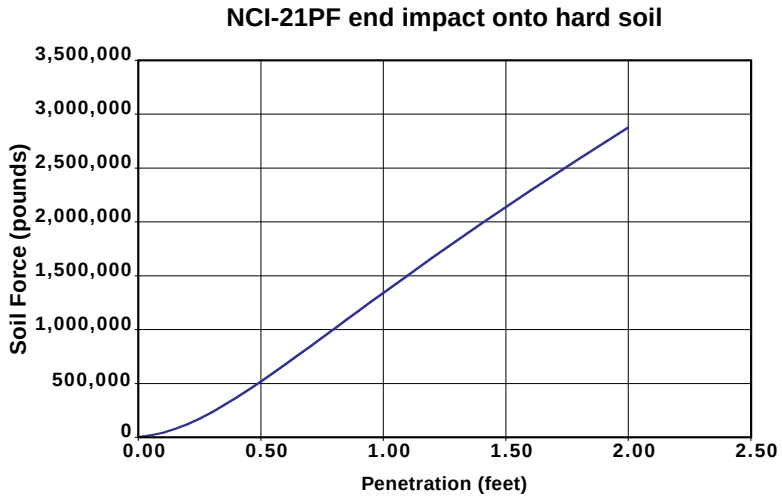

Figure 6.3 - Force-deflection Curve for Hard Soil impacted by a 43-inch diameter Package

orientation, an equivalent package diameter was used to calculate the soil force-deflection curve. For end-on impacts the actual package diameter (43 inches) is used. For corner impacts, as soon as the package penetrates a few inches the entire end of the package is resisted by soil, so again the actual package diameter was used. For side impacts, after a few inches of penetration the entire package area is resisted by soil. An equivalent diameter is determined such that a circle with that diameter has the same area as the surface of the package that is contacting the soil. For the 21PF this diameter is 72 inches.

Once the force-deflection curves for each soil type and package orientation have been developed, the amount of energy absorbed by the soil can be calculated. The absorbed energy for a given penetration depth is equal to the integral of the force-deflection curve up to that penetration depth. For each curve a numerical integration is performed and absorbed energy is plotted versus peak contact force. Figure 6.4 shows this curve for the end-on impact on hard soil. Using these curves, the amount of energy absorbed by the soil for any peak contact force can be determined. Table 6.1 shows the energy absorbed by the soil for end, corner, and side impacts onto hard, stiff, medium, and soft soils. This approach is valid as long as the cross sectional area of the package does not change appreciably due to the impact.

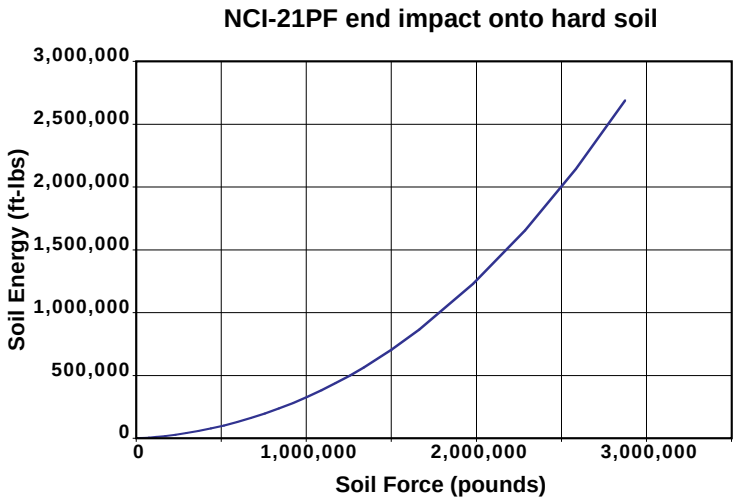

Figure 6.4 - Energy-Force Curve for Hard Soil impacted by a 43-inch diameter Package

Table 6.1- Energy Absorbed by Soil Targets (ft-lbs)

Soil Type	Number of Blows	End (F=2.6E6 lbs)	Corner (F=1.5E6 lbs)	Side (F=1.5E6 lbs)
Hard	30	2.17E+06	7.05E+05	4.41E+05
Stiff	12	5.74E+06	1.90E+06	1.06E+06
Medium	6	1.35E+07	4.21E+06	2.33E+06
Soft	3	2.87E+07	9.13E+06	5.11E+06

The energy absorbed by the soil is added to the initial kinetic energy of the package (the energy absorbed by the package during an impact on an unyielding target) to derive a new kinetic energy for an equivalent impact on a yielding target. From this kinetic energy, an equivalent velocity is calculated. Table 6.2 shows the equivalent velocities for each of the soil types in Table 6.1.

Table 6.2 - Velocity for Soil Target Impacts (mph) Equivalent to 30 mph Regulatory Impact

Soil Type	End	Corner	Side
Hard	130	78	65
Stiff	208	122	94
Medium	318	179	135
Soft	462	262	197

6.2.2 Impacts on Concrete Slabs

The severity of an impact on a concrete target depends on the thickness of the concrete, the size and stiffness of the package, and the impact velocity. A limited amount of data for package impacts faster than 30 mph on concrete targets is available [6.4]. Concrete targets resist penetration in two ways. First is by the shear stiffness of the concrete itself. After the concrete slab fails in shear, further penetration is resisted by the stiffness of the sub-grade material beneath the slab. For UF_6 packages, the peak contact force is sufficient to generate a shear failure in the slab, but little or no further penetration. Table 6.3 gives the energy absorbed by slabs of 6-in, 9-in, 12-in, and 18-in thickness for impacts in the end, corner, and side orientations (interface forces in parentheses).

Table 6.3 - Energy Absorbed by Concrete Slabs (ft-lbs)

Slab Thickness	End (F=2.6E6 lbs)	Corner (F=1.5E6 lbs)	Side (F=1.5E6 lbs)
6 inches	1.63E+05	5.42E+04	3.22E+04
9 inches	8.01E+04	2.67E+04	1.58E+04
12 inches	4.84E+04	1.61E+04	9.56E+03
18 inches	2.38E+04	7.93E+03	4.70E+03

In the same way as for the soil targets, these amounts of energy absorbed in the target are transformed into the equivalent impact velocities given in Table 6.4. As can be seen from the table, for the thicker slabs the equivalent velocity is not much higher than the unyielding target velocity. For UF_6 packages, concrete slabs greater than 12-inches thick are nearly unyielding.

Table 6.4 - Velocity for Concrete Slab Impacts (mph) Equivalent to 30 mph Regulatory Impact

Slab Thickness	End	Corner	Side
6 inches	46	36	34
9 inches	39	33	32
12 inches	35	32	31
18 inches	33	31	31

6.2.3 Impacts on Rock Targets

There is a range of stiffness for exposed rock faces. In much of the country, the exposed rock is weathered sedimentary rock. This type of rock (soft rock) is only slightly stiffer than hard soil. To determine impact velocities, that produce the same amount of damage as the regulatory impact on an unyielding target, for this type of rock, the forces obtained for hard soil impacts were doubled. This is equivalent to 60 blows on a cone penetrometer rating system used for soils.

In some areas of the country there are exposed rock surfaces that are nearly unyielding, i.e. sufficiently stiff to approximate an unyielding target for a UF_6 package. Table 5 gives the equivalent impact velocities for impacts onto rock surfaces.

Table 6.5 - Velocity for Rock Target Impacts (mph) Equivalent to 30 mph Regulatory Impact

Surface	End	Corner	Side
Hard Rock	30	30	30
Soft Rock	94	61	53

6.2.4 Impacts by Trucks

Truck impacts can occur in several ways. The truck carrying the package can be involved in a head-on collision with another truck, the truck carrying the package can be struck from behind by another truck, the vehicle carrying the package can be hit in the side by a truck, or a package that has come off of the trailer in an accident can be struck directly by a truck. In the first three of these scenarios, a portion of the energy of the collision will be absorbed by the vehicle carrying the UF_6 package. This will mitigate the severity of the impact, so it will be less severe than the fourth scenario. Therefore, to be conservative, it will be assumed that all truck impacts are directly on the UF_6 package. The severity of an impact directly on a package by a truck is limited by the amount of force the truck can apply to the package. Figure 6.5 shows the accelerations for a ¼-scale impact test, conducted by Sandia [6.7], in which a tractor-trailer rig impacted an unyielding target at 53.5 mph. To convert this acceleration trace to acceleration for a full-scale package, the accelerations must be divided by four and the times multiplied by four. Numerical integration of the acceleration trace gives the velocity as a function of time. Numerical integration of the velocity gives displacement. The contact force between the truck and the unyielding target is obtained by multiplying the accelerations by the mass of the truck. Figure 6.6 shows the resultant force-deflection curve for the impact.

The peak contact force between the tractor-trailer and the unyielding target is about 1,500,000 pounds. This force is from the entire frontal area of the tractor impacting the unyielding target. If a truck were to impact a UF_6 package, only a portion of the frontal area would be involved in the collision, so the amount of force that could be generated would be less than that shown in Figure 6.6. The peak contact force for the 30 mph impact of the UF_6 package on an unyielding target is therefore greater than the amount of force that a truck can apply to the package. If we assume that the truck absorbs the amount of energy associated with the UF_6 package impacting it at 53.5 mph, the equivalent velocity for an unyielding target impact is 61 mph. Because the force the truck is able to apply to the package is actually less than the force required to produce the damage associated with the regulatory impact, this equivalent velocity is conservative.

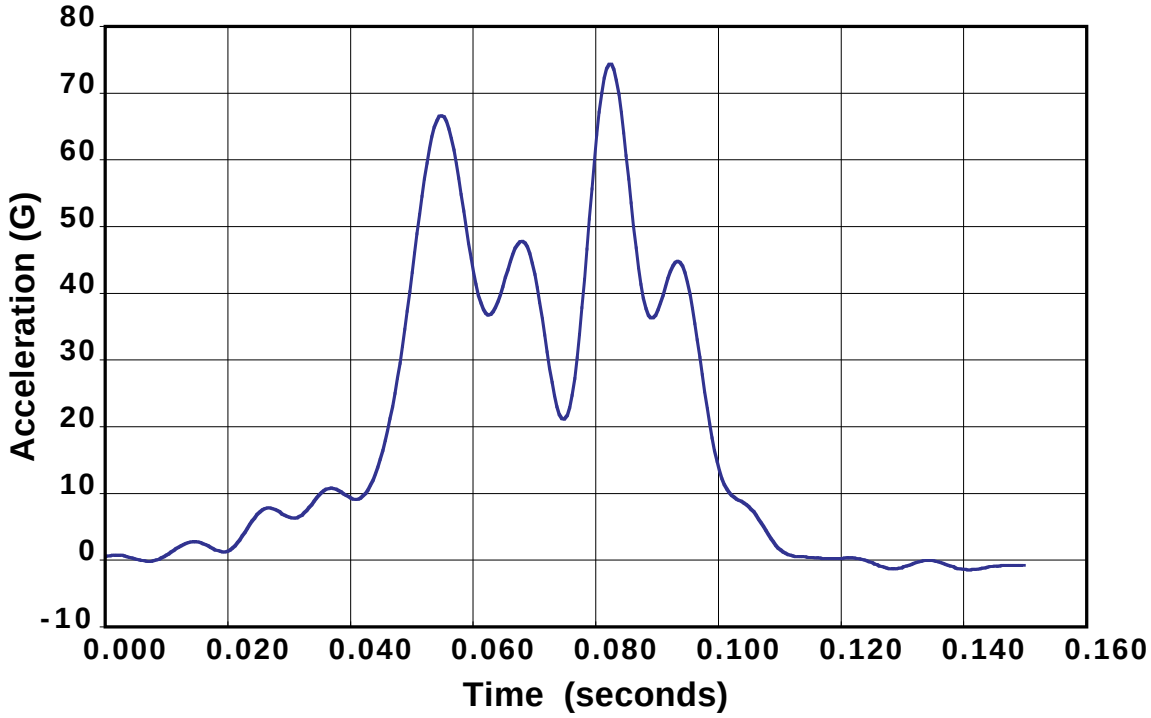

Figure 6.5 - Acceleration Trace for a 1/4-scale Tractor-Trailer Impacting an Unyielding Target

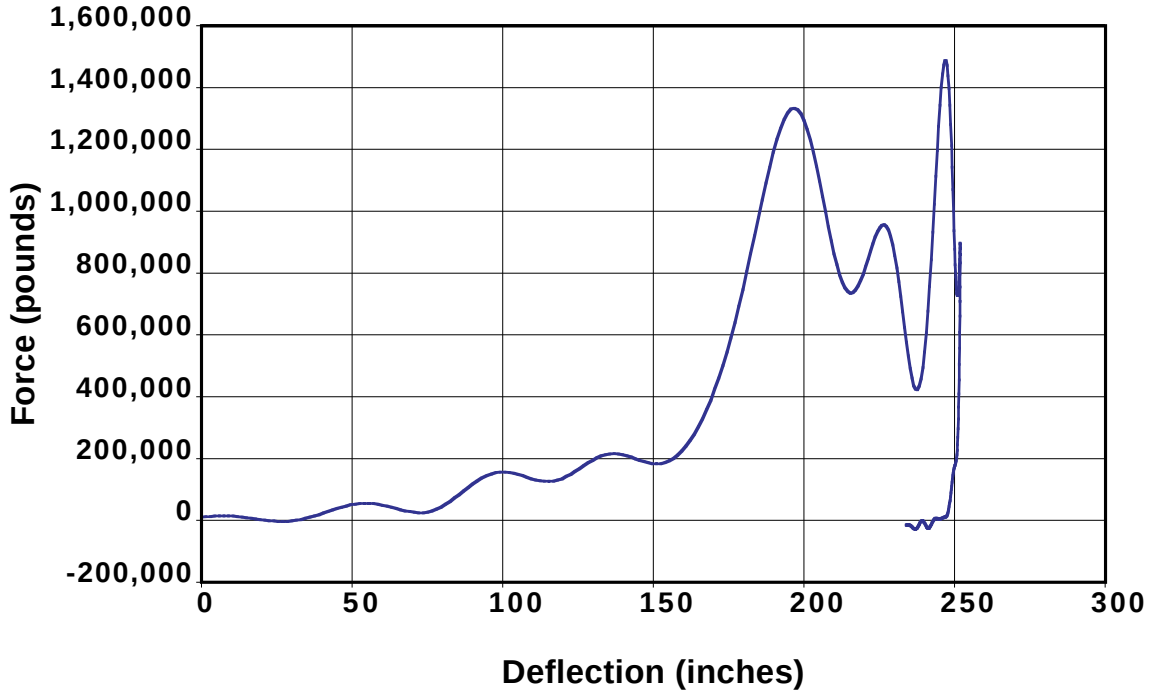

Figure 6.6 - Derived Full-scale Tractor-trailer Force-deflection Curve

6.2.5 Impacts by Trains

For this accident case, only grade crossing accidents, in which a train impacts the side of the truck carrying the UF_6 package, will be considered. Other types of grade crossing accidents are much less severe and are therefore neglected. For containers transported axially on a truck, the train impact will be on the side of the container. During the 1970s, Sandia performed a test in this configuration with a locomotive impacting a spent fuel cask on a flat-bed trailer at a speed of 81 mph. The cask and locomotive positions were determined at each frame of the high-speed film. The cask position information was used to generate an acceleration time history. Multiplication of these accelerations by the mass of the cask gives a force time history. The difference in position between the cask and the locomotive was used to determine the amount of locomotive crush. Figure 6.7 shows the resulting force-deflection curve for the locomotive derived from the data. The maximum force was about 1,800,000 pounds, which is slightly higher than the force exerted on the UF_6 container in the regulatory side impact. The energy absorbed by the train in reaching a force of 1,500,000 pounds is 1,720,000 ft-lbs. For a perfectly plastic collision between a train and a UF_6 container, the amount of energy that must be absorbed between the two bodies can be calculated from conservation of momentum and conservation of energy. This amount of energy is proportional to the initial energy of the train. To get a train impact velocity that is equivalent to the regulatory impact test, the absorbed energy from the perfectly plastic collision must be equal to the energy absorbed by the UF_6 container in the regulatory impact test plus the energy absorbed by the locomotive in reaching the same contact force. Solving this equation gives an equivalent impact velocity of 117 mph.

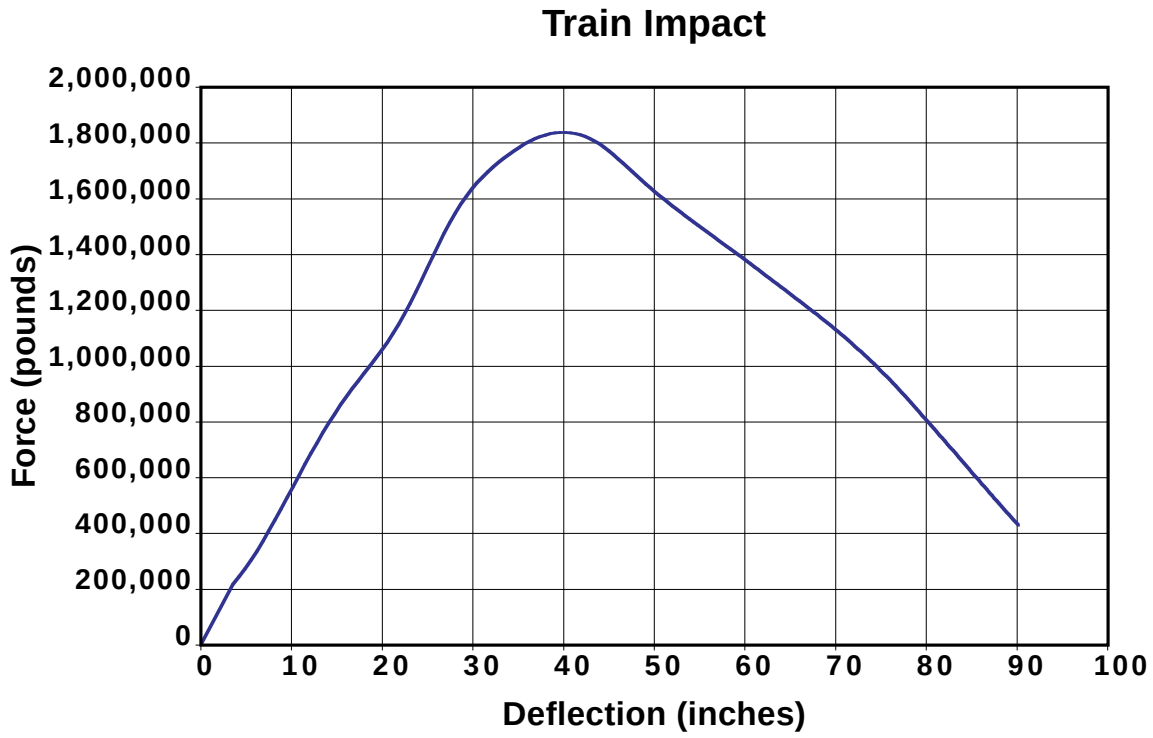

Figure 6.7 – Force-Deflection Curve for a Train Impacting a Spent Fuel Cask

7.0 THERMAL ANALYSIS

Three UF_6 packages were examined for this study. These were the UX-30 [2.2], ESP-30X [2.3], and NCI-21PF-1 [2.1]. From these, the UX-30 was selected as the reference package to build the finite element model (FEA). The overall dimensions of the FEA model that was built for this study are shown in Figure 7.1. The MSC PATRAN/Thermal [7.1] computer code was used to generate the model and run the thermal calculations. A section of the finite element model of the UX-30 package is presented in Figure 7.2. In this model, the UX-30 packaging with the carbon steel 30B cylinder and the UF_6 content is represented by 5,836 three-dimensional finite elements. This model was then used for the simulation of all the cases that were described above by applying the appropriate boundary conditions.

The 30B cylinder was assumed to be co-centric with the UX-30 overpack. The uniform 0.375-in. air gap shown in Figure 7.2 allows radiation exchange between the inner wall of the UX-30 overpack and the outer wall of the 30B cylinder. A view factor of one was assumed as well as emissivity values of 0.5 and 0.8 for the stainless steel inner wall of the UX-30 and the outer wall of the 30B cylinder, respectively. This radiation exchange was included in all the thermal simulations that are discussed in this analysis. The material properties used in this model were the same as those presented in the SAR for the UX-30 overpack, including the emissivity values mentioned above. The UF_6 was not assumed to generate any significant decay heat. As shown in Figures 7.1 and 7.2, the 30B cylinder was assumed to be completely full of UF_6 and its ends are as far from the overpack inner wall as the sides. In other words, the valve region and the bottom region where the cylinder would sit if it were positioned vertically were not included in the model, i.e. the UF_6 is modeled as closer than the actual distance from the overpack inner wall. Therefore, the temperature results for the UF_6 near the ends of the overpack are expected to be conservative values. Finally, the stainless steel skin that protects the polyurethane foam on the UX-30 overpack was modeled by a thickness of 0.236 in. and the walls of the 30B cylinder were modeled as 0.5 in. thick.

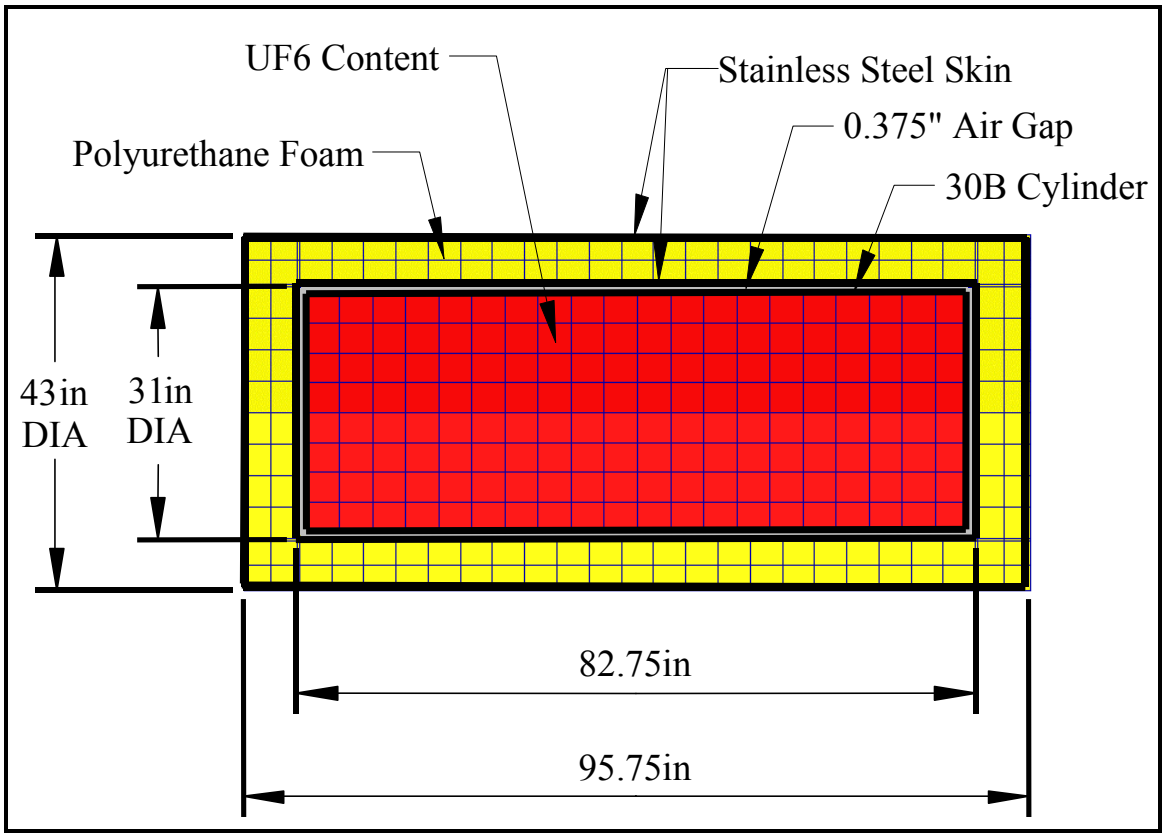

Figure 7.1 - Overall Dimensions of Modeled UX-30 Package

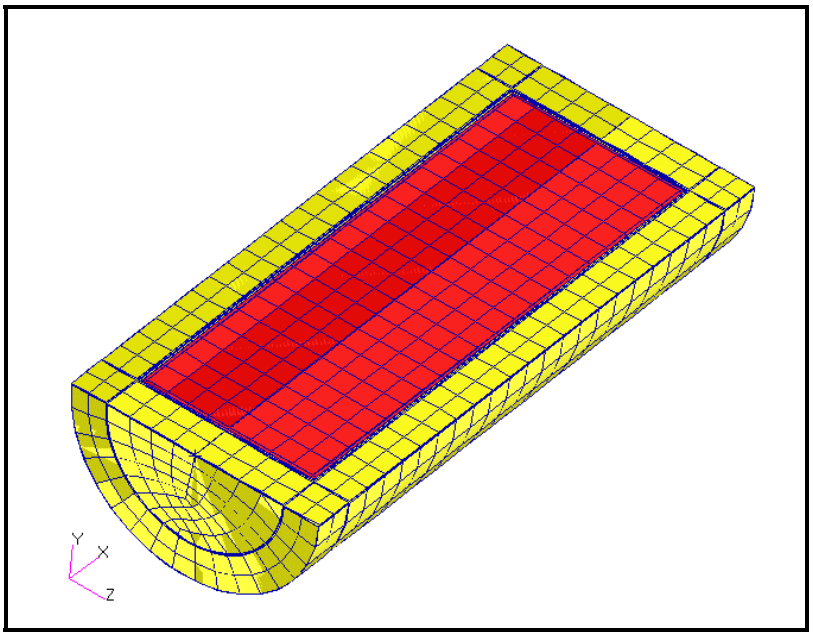

Figure 7.2 - 3D FEA Model of the UX-30 Package (bottom half).

7.1 Normal Transport Conditions

In the Safety Analysis Report (SAR) for the UX-30 package, the only results presented for an undamaged package were those for the normal transport conditions. Therefore, a simulation of these conditions was performed with the model developed for this study in order to compare the results to those published in the SAR. The boundary conditions used (same as those in the SAR) are summarized in Table 7.1. The results of the steady-state simulation are presented in Figure 7.3; a comparison with the results reported in the SAR is presented in Table 7.2.

Table 7.1 - Boundary Conditions for Normal Transport

Boundary Condition	Application Region	Value
Insolation (Solar irradiation)	Curved surface $0 \leq \theta \leq 180°$	193.9 W/m^2 in a 12-hr period
	Vertical flat surfaces	96.95 W/m^2 in a 12-hr period
Natural convection	All external surfaces of UX-30	3.64 W/m^2-K
Radiation to environment	All external surfaces of UX-30	Surface emissivity of 0.5
Environment temperature	N/A	38°C

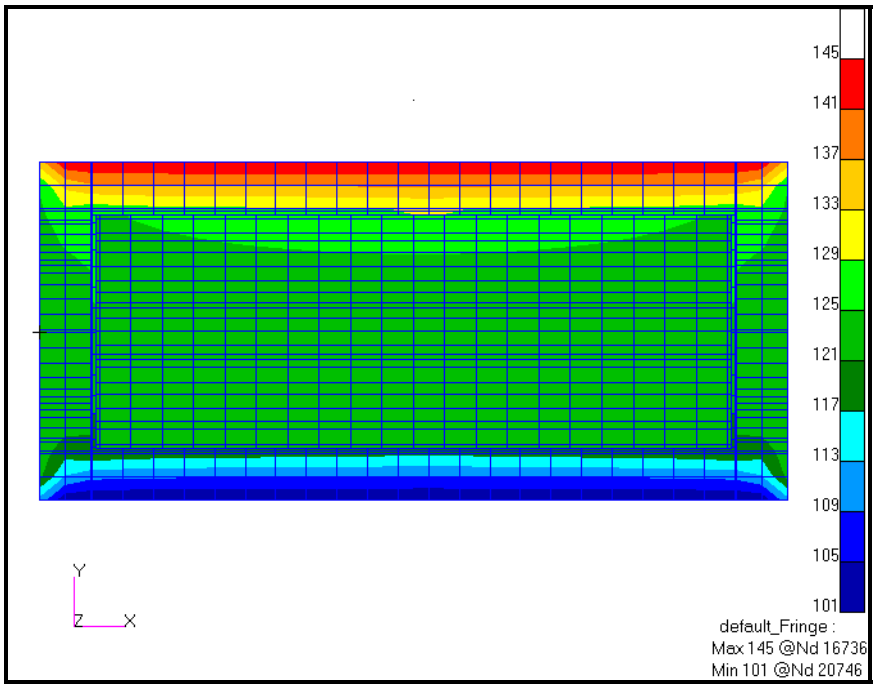

Figure 7.3 - Cross-Sectional View of the Steady-State Solution for Normal Transport Conditions (°F)

Table 7.2 - Comparison of the Steady-State Solutions

Location	Temperature (°F)	
	UX-30 SAR	Current Analysis
Top outer surface of the UX-30	145.3	145.7
Top inner surface of the UX-30	125.7	129.6
Top of 30B cylinder	124.0	126.1
Closure interface at the outer surface	125.4	125.0
Closure interface at the inner surface	121.7	124.3
UF_6	124.0	124.1

As illustrated in Table 7.2, the results for normal transport conditions from the current model are very similar to those that are reported in the SAR for the UX-30. These results confirm the adequacy of the current model to predict the thermal performance of the UF_6 package.

7.2 Regulatory Accident Conditions

In order to determine how long it takes for fire environments other than the regulatory environment described in 10 CFR Part 71 [1.1] to present a similar threat to the undamaged UF_6 package, the regulatory accident conditions had to be modeled. The boundary conditions imposed on the exterior of the cask are presented in Table 7.3. The results from this simulation are presented in Figures 7.4 and 7.5. Note that the peak temperature of the UF_6 occurred after heating by the fire had ceased.

Table 7.3 - Hypothetical Accident Boundary Conditions Used

Boundary Condition	Application Region	Value
Temperature of environment	External node	800°C for the first 30 min. and 38°C after fire cessation
Radiation exchange between the cask and the environment	Outer surface of UX-30	Surface emissivity of 0.8*
	Fully-engulfing fire	Surface emissivity of 0.9
	View factor	1
Convection during the fire	All external surfaces of UX-30	Heat transfer coef. of 22.7 W/m^2-K
Convection after the fire	All external surfaces of UX-30	Heat transfer coef. of 3.64 W/m^2-K

* Emissivity is higher due to soot deposition in the fully engulfing fire

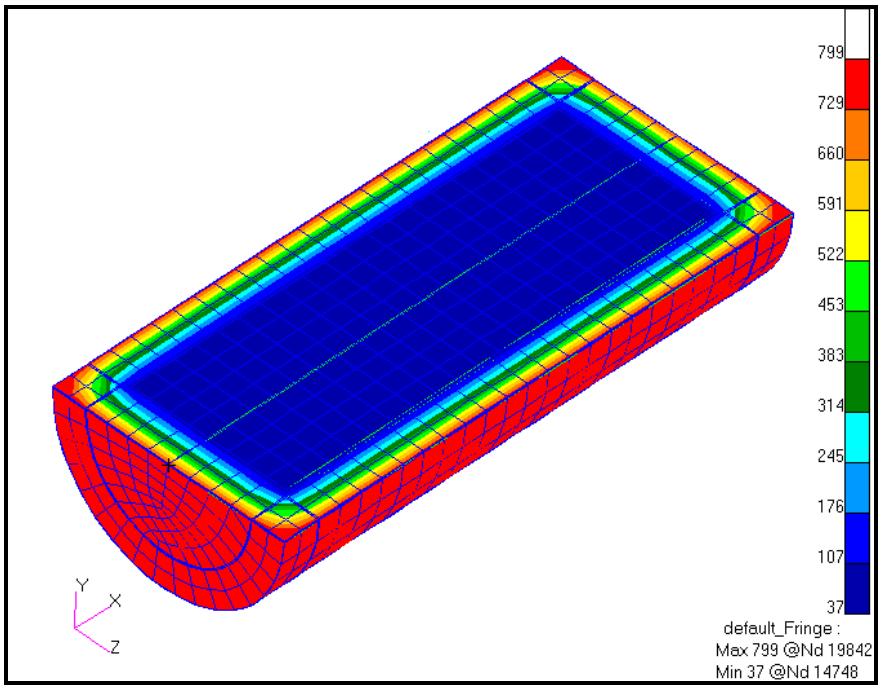

Figure 7.4 - Temperature Distribution for the 10 CFR Part 71 Simulation (temperatures in °C)

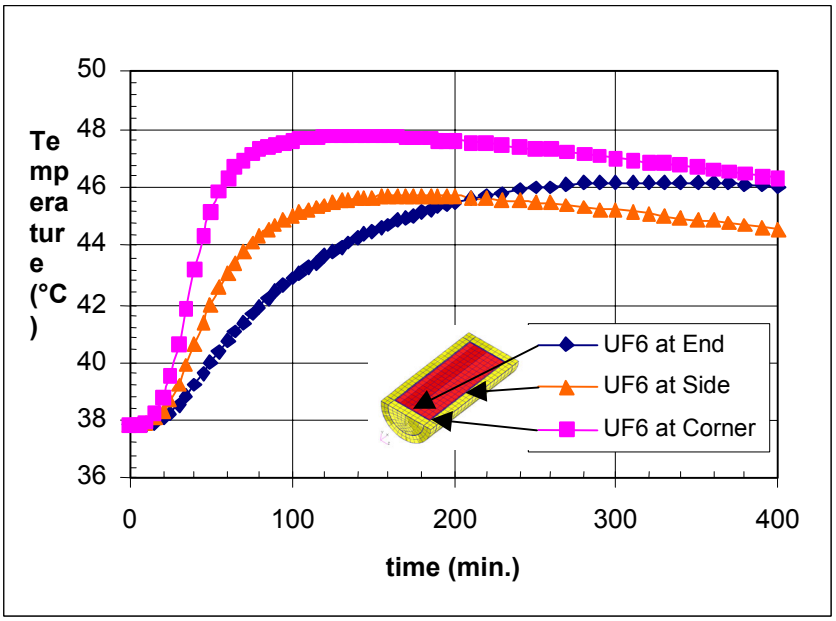

Figure 7.5 - Temperature History of Three Outer Boundary Points of the UF_6

As shown in Figure 7.5, the temperature of the corner node heated the fastest due to the fact that heat is entering the corner from the side and the end simultaneously. On the other hand, only the temperatures of the end and the side will be considered in this study

since they are a better representation of the bulk temperature of the UF_6 at the boundaries. The maximum temperature of the UF_6 at the side and the end in this simulation will be used as thresholds to determine equivalent conditions in the following analyses.

7.3 UF_6 Package Away from a Fire

Four simulations, in the configurations described earlier were performed. A top view of the package and fire positions is illustrated in Figure 7.6, and the trapezoidal surface used to represent the fire in the model in shown in Figure 7.7. The boundary conditions used for the two simulations with the package one meter away from the fire were the same except for the location of the fire; these conditions are presented in Table 7.4. Table 7.5 lists the boundary conditions used for the simulations in which the fire was five and ten meters away from the side of the cask.

Note that the diameter of the assumed fire extends to the maximum recommended pool fire diameter according to 10 CFR Part 71 relative to the length of the package. That is, three meters from the outer surface of the package to the edge of the pool. In reality, an oval or rectangular pool would be necessary in order not to exceed this limit when measured from the side of the package, but for the purpose of this study, the pool was assumed to be circular, allowing the boundary of the fire to extend 0.66 m further beyond the cask diameter.

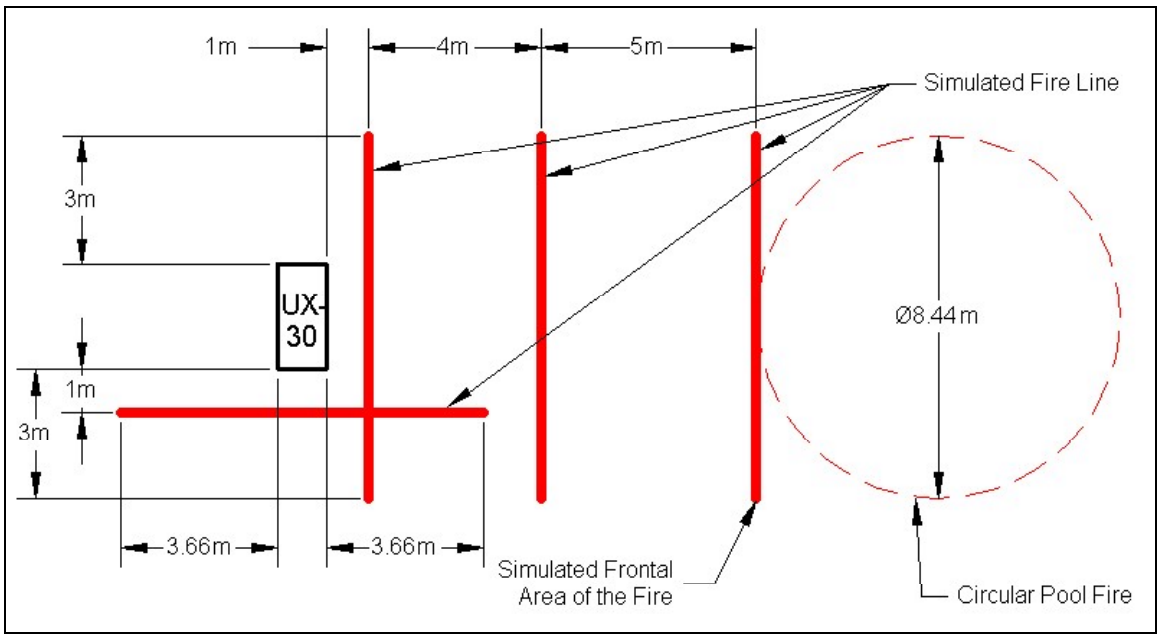

Figure 7.6 - Top View of the Four Scenarios Modeled

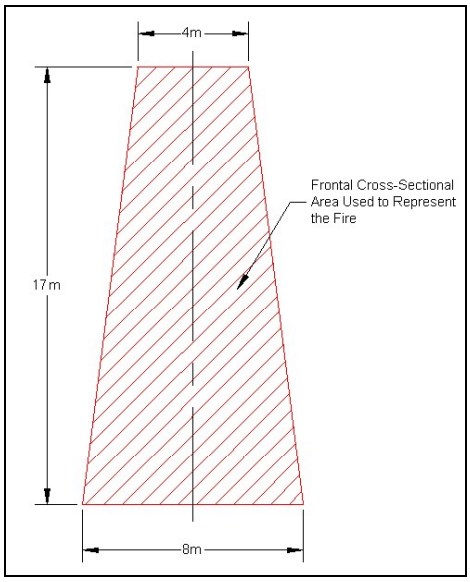

Figure 7.7 - Surface used in the FEA Model to Represent the Fire (dimensions to nearest meter)

This will introduce some conservatism, relative to the slightly smaller fire diameter, in the calculation of the package response when one of its ends was directly exposed to the fire. The height of the fire was assumed to be two pool diameters, which is typical of open pool fires.

Table 7.4 - Boundary Conditions Used for Fire 1 Meter Away

Boundary Condition	Application Region	Value
Fire temperature	External node	800°C for 400 minutes
Environment temperature	External node	38°C
Radiation exchange between the cask and the fire	Outer surface of UX-30	Surface emissivity of 0.5
	Fire surface	Surface emissivity of 0.9
	View factor	Position dependent (calculated by P/Thermal)
Insolation (Solar irradiation)	Curved surface $0 \leq \theta \leq 180°$	Heat transfer coef. of 193.9 W/m^2
	Vertical flat surfaces	Heat transfer coef. of 96.95 W/m^2
Natural convection	All external surfaces of UX-30	Heat transfer coef. of 3.64 W/m^2-K

Table 7.5 - Boundary Conditions Used for Fire 5 and 10 Meters Away

Boundary Condition	Application Region	Value
Fire temperature	External node	800°C for 400 minutes
Environment temperature	External node	38°C
Radiation exchange between the cask and the fire	Outer surface of UX-30	Surface emissivity of 0.5
	Fire surface	Surface emissivity of 0.9
	View factor	Position dependent (calculated by P/Thermal)
Radiation from the cask to the environment	Outer surface of UX-30	Surface emissivity of 0.5
		Environment emissivity of 1
	View factor	1
Insolation (Solar irradiation)	Curved surface $0 \leq \theta \leq 180°$	Heat transfer coef. of 193.9 W/m^2
	Vertical flat surfaces	Heat transfer coef. of 96.95 W/m^2
Natural convection	All external surfaces of UX-30	Heat transfer coef. of 3.64 W/m^2-K

7.3.1 Package one meter away from the fire

The two simulations in which the package was one meter away from the fire used the boundary conditions presented in Table 7.4. The results of these simulations at 30 minutes are presented in Figures 7.8 and 7.9.

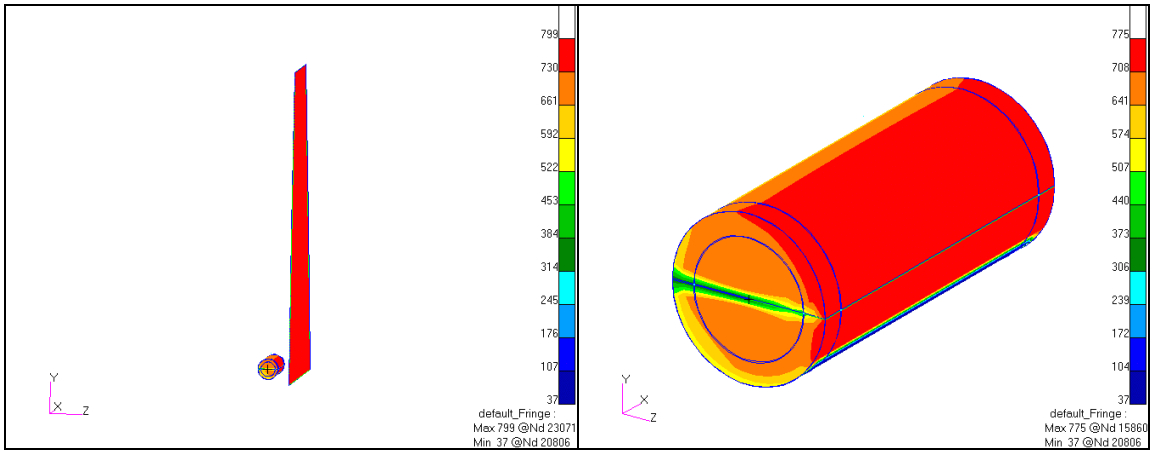

Figure 7.8 - Temperature Distribution at 30 min., Side of Package 1m from the Fire (°C)

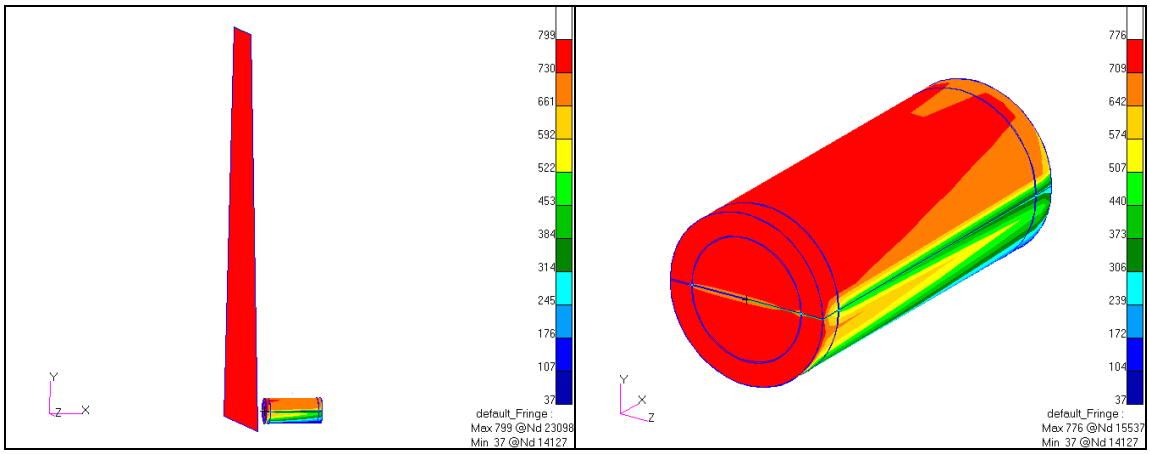

Figure 7.9 - Temperature Distribution at 30 min., End of Package 1m from the Fire (°C)

7.3.2 Package five and ten meters away from the fire

The two simulations in which the package was five and ten meters away from the fire used the boundary conditions presented in Table 7.5. The results of these simulations at 30 minutes are presented in Figures 7.10 and 7.11.

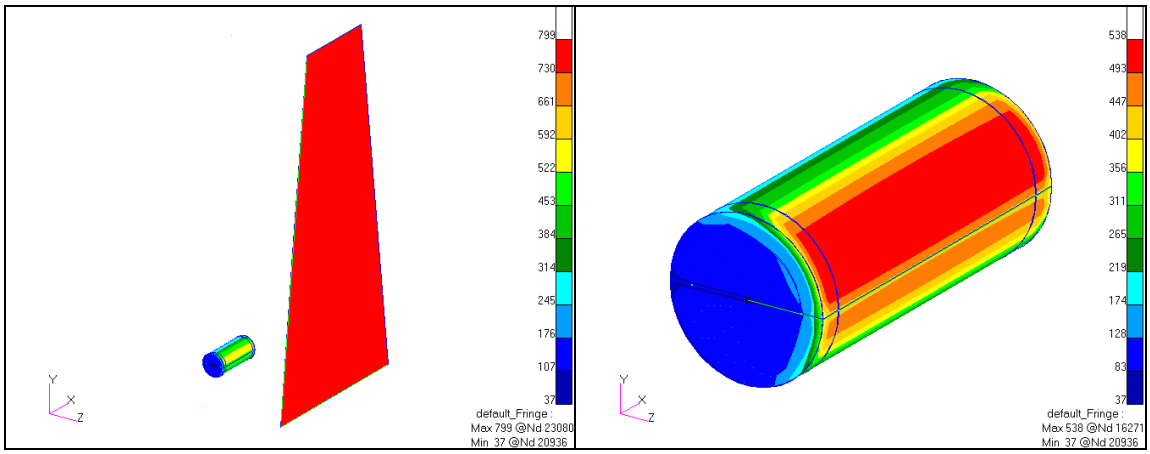

Figure 7.10 - Temperature Distribution at 30 min., Side of Package 5m from the Fire (°C)

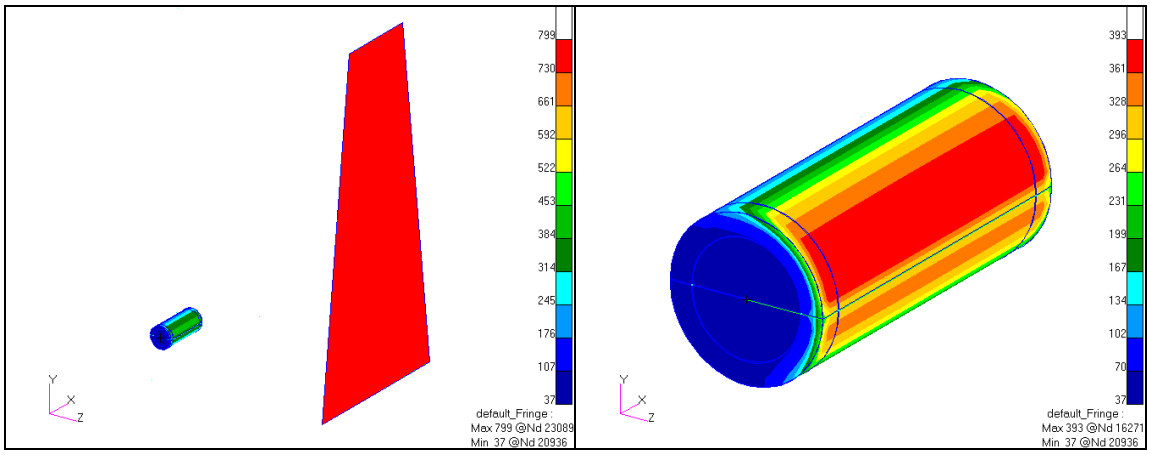

Figure 7.11 - Temperature Distribution at 30 min., Side of Package 10m from the Fire (°C)

7.3.3 Summary of Simulations

The temperature history records of all the transient simulations are compared to the temperature reached in the 30 min. regulatory fire (45.73 °C and 46.21 °C) in Figures 7.12 and 7.13 . Figure 7.12 presents the results for the UF_6 temperature on the side of the package whereas Figure 7.13 presents the results for the UF_6 temperature on the end of the package.

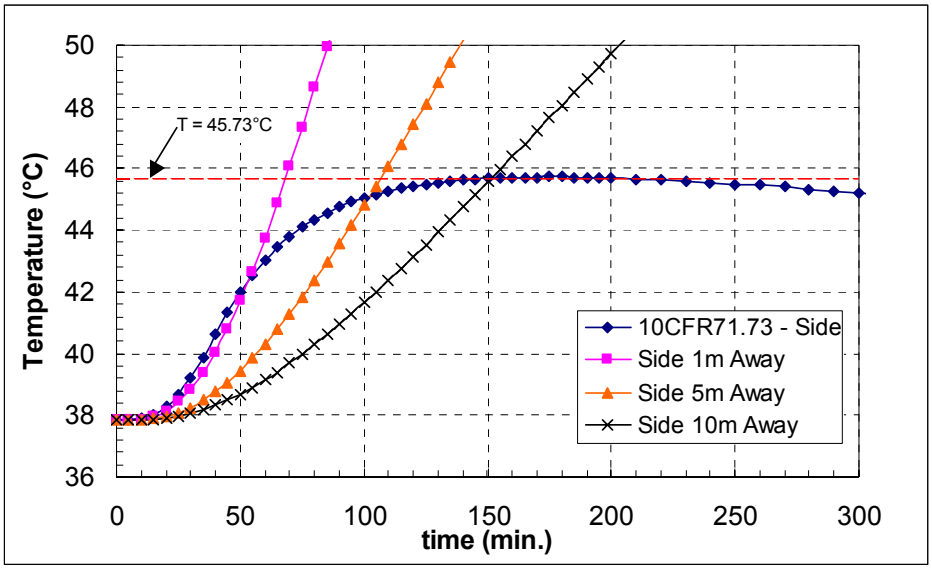

Figure 7.12 - Comparison of Time-to-Threshold of UF6 Temperature, Side of the Package

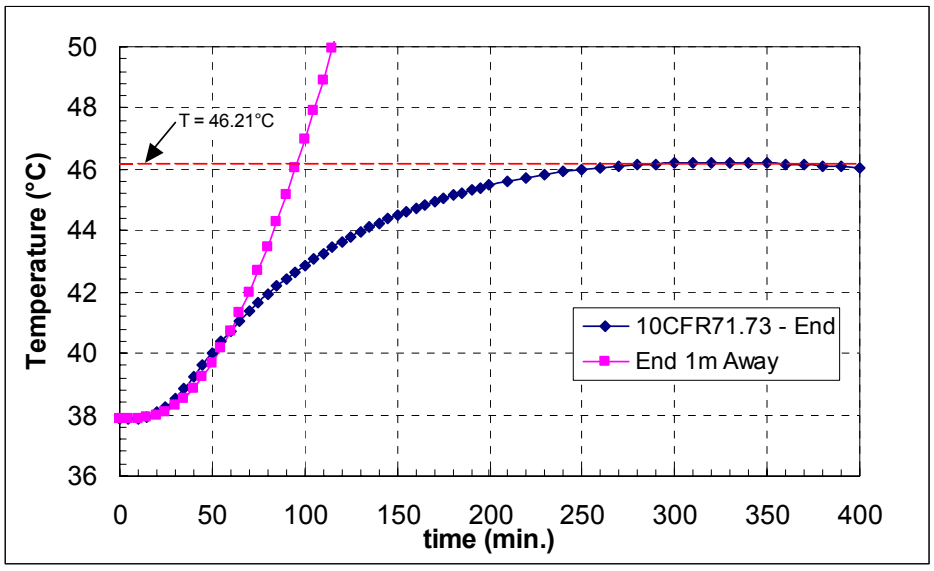

Figure 7.13 - Comparison of Time-to-Threshold of UF6 Temperature, End of the Package

Note that the maximum temperature observed from the 10 CFR Part 71 simulation was 45.73°C for the UF_6 on the side and 46.21°C for the UF_6 at the end of the package. These temperatures were the threshold temperatures used to determine the time at which the other scenarios pose a similar threat to the UF_6. Table 7.6 lists the times (as defined by the finite time-steps of the simulation) at which these temperatures (or closest calculated values) were reached for each of the transient simulations.

Table 7.6 - Threshold Temperatures and Times

Simulation	Temperature (°C)	Time (min.)
10 CFR 71 - Side	45.73	175
Side 1m Away	46.06	69
Side 5m Away	46.10	107
Side 10m Away	45.98	152
10 CFR 71 - End	46.21	310
End 1m Away	46.97	96

It is important to understand that these simulations were performed under the assumption that the overpack was undamaged. Also, in the non-regulatory cases, the fire was assumed to burn continuously. In reality, these non-regulatory fires could burn for shorter times and still reach the temperature thresholds defined by the regulatory simulation. Shorter fire burn-times would, in turn, yield higher probabilities of occurrence.

8.0 RESULTS

For each end-point in Figure 4.1, the fractional occurrence was multiplied by a fraction representing the probability of the corresponding accident speed, as defined by speed probability distributions in NUREG/CR-6672 [1.2] and threshold values in Section 6.0 (displayed in Table 8.1). Fire duration probabilities determined from probability distributions in NUREG/CR-6672 and thresholds developed in Section 7.0 are listed in Table 8.2. The probability distributions from NUREG/CR-6672 are tabulated in that document as cumulative probabilities, i.e. probability (P_c) of a threshold or smaller value being reached. In Tables 8.1 and 8.2, the complement of that value ($1 - P_c$), i.e. the probability that the threshold value will be exceeded, is used; this yields a conservative estimate of the probability that the regulatory conditions are exceeded. Total probabilities of exceeding regulatory thresholds for specific accident types and fire scenarios of interest are computed by multiplication of a probability from Table 8.1, the probability that an accident occurs (Table 5.1), the probability that a fire occurs (0.018), and the probability of a specific fire scenario from Table 8.2.

The combinations of probabilities in Table 8.1 and fire-scenario probabilities in Table 8.2 can be modified further by the probabilities for special circumstances leading to immersion of the package in water or intrusion of water into the inner cylinder, discussed in Sections 4.1-3. The probability of water being applied to a fire by first-responders was estimated to be 50%; a factor of 0.5 could conceivably apply to any of the scenarios since there is a finite probability of fire for each case. The probability that water could enter the cylinder as a result of heavy rainfall, 8E-6, can apply to the scenarios in Table 8.1 because the speed probabilities include values greater than the thresholds, leading to a small probability of damage to the fill-valve for each scenario except fire-only. Finally, for each of the hypothetical routes listed in Table 8.1, the corresponding fraction of the route bordering or over water may be applied to the total probabilities in Table 8.1 for "Off road" scenarios to estimate (very conservatively) the probability of immersion of the package in water. All of the probabilities in these three categories of exposure to water indicate a further reduction, below the small likelihood of accidents exceeding the regulatory conditions, for the probability of any special consequences relating to such exposures to water. The following example illustrates this procedure:

> For the suburban portion of the route from Portsmouth, OH, to Wilmington, NC, the probability of an accident in which the shipment runs off the road and over an embankment, to impact hard soil at a speed equivalent to the regulatory limit is:
>
> $Prob_{Accid} = (409)(3E\text{-}7)(1.3E\text{-}5) = 1.6E\text{-}9$
>
> If the package careens into a nearby body of water, the probability of an immersion accident is:
>
> $Prob_{Imm} = 1.6E\text{-}9(0.07) = 1.1E\text{-}10$
>
> If, instead, there is a fire (1 meter from the package side, lasting for the equivalent of a regulatory fire) after the impact on hard soil:
>
> $Prob_{Fire} = 1.6E\text{-}9(0.018)(0.0002) = 5.8E\text{-}15$

Table 8.1 – Probabilities of Exceeding Regulatory Speed Equivalents for 31 Accident Scenarios

Event Tree Scenario	Num.	Scenario Probability	Speed Probability	Total Probability
Collisions, Non-fixed Objects				
Cones, pedestrians, etc.	1	0.03400	0.0	**0.0**
Motorcycle	2	0.00809	0.0	**0.0**
Automobile	3	0.43152	0.0	**0.0**
Truck, bus	4	0.13320	0.018	**0.0024**
Train	5	0.00770	1.0E-5	**7.7E-8**
Other	6	0.03811	0.0	**0.0**
Collisions, On-road Fixed Objects				
Bridge Rail., Water	7	0.00104	0.0	**0.0**
Bridge Rail., Railb. or Roadb.	8	0.00399	0.58	**2.3E-3**
Bridge Rail., Clay or Silt	9	0.00008	1.1E-6	**8.8E-11**
Bridge Rail., Hard S. or Soft R.	10	4.0E-6	0.018	**7.2E-8**
Bridge Rail., Hard Rock	11	3.0E-6	0.72	**2.2E-6**
Small Column	12	0.00030	0.0	**0.0**
Large Column	13	0.00006	0.0051	**3.1E-7**
Abutment	14	0.00001	0.17	**1.7E-6**
Concrete Object	15	0.00085	0.0	**0.0**
Barrier, Wall, Post	16	0.04008	0.0	**0.0**
Signs	17	0.00511	0.0	**0.0**
Curb, Culvert	18	0.03705	0.0	**0.0**
Non-collisions, Off-road				
Slope, Clay or Silt	19	0.02297	1.1E-6	**2.5E-8**
Slope, Hard S. or Soft R.	20	0.00126	0.0097	**1.2E-5**
Slope, Hard Rock	21	0.00101	0.26	**2.6E-4**
Embankment, Clay or Silt	22	0.01314	1.1E-6	**1.4E-8**
Embankment, Hard S. or Soft R.	23	0.00072	0.018	**1.3E-5**
Embankment, Hard Rock	24	0.00058	0.72	**4.2E-4**
Embankment, Drainage Ditch	25	0.00889	0.0	**0.0**
Trees	26	0.00941	0.0	**0.0**
Other	27	0.03252	0.0	**0.0**
Non-collisions, Other				
Overturn	28	0.08349	0.0	**0.0**
Jackknife	29	0.05460	0.0	**0.0**
Other mechanical	30	0.02050	0.0	**0.0**
Fire Only	31	0.00970	1.0	**9.7E-3**

Table 8.2 – Probabilities of Fire Exceeding the Regulatory Temperature Equivalents (Average Fire Occurrence = 0.018)

Fire Scenario	Time to Temp. (minutes)	Non-Collision Accidents	Off-Road Accidents & Fixed-Object Collisions	Truck Collisions	Train Accidents
Side Exposure 1 meter Away	69	0.00004	0.0002	0.15	0.10
Side Exposure 5 meters Away	107	0.0	0.0	0.12	0.068
Side Exposure 10 meters Away	152	0.0	0.0	0.090	0.045
End Exposure 1 meter Away	96	0.0	0.0	0.13	0.076

If, in addition, first-responders fight the fire with water, the probability of this accident consequence is:

$Prob_{Water} = 5.8E\text{-}15(0.5) = 2.9E\text{-}15$

Note that all of these probabilities are per shipment.

Examination of the results in Tables 8.1 and 8.2 indicate that the probabilities of exceeding regulatory conditions in accidents of the various types defined by the event tree (Figure 4.1), and by structural and thermal analyses of possible conditions resulting from such accidents, reveals a limited number of circumstances under which regulatory conditions may be exceeded. Furthermore, their probabilities are small, i.e. the likelihood of UF_6 being dispersed by impact or fire is small while the probability that accidents will lead to conditions within the regulatory limits is substantial. Similarly, applying the probabilities of further consequences resulting from exposure to water by fire-fighting, heavy rain or off-road excursion into a body of water leads to even lower probabilities, by factors ranging from 0.5 to 8E-6.

9.0 References

1.1 U.S. Nuclear Regulatory Commission, Code of Federal Regulations, Title 10, Part 71

1.2 Sprung, J. L., et al., "Reexamination of Spent Fuel Shipment Risk Estimates," NUREG/CR-6672, Sandia National Laboratories, Albuquerque, NM. (2000)

1.3 Fischer, L. E., et al., "Shipping Container Response to Severe Highway and Railway Accident Conditions," NUREG/CR-4829, Lawrence Livermore National Laboratory, Livermore, CA. (1987)

2.1 Transnuclear, Inc., Safety Analysis Report for the NCI-21PF-1 Protective Shipping Package, Revision 2, COC 71-9234, Transnuclear, Inc., Hawthorne, NY, 1997 (available from NRC public document room)

2.2 Chem-Nuclear Systems, Safety Analysis Report for the UX-30 Packaging, Revision 0, COC 71-9196, UX-30 Consolidated SAR, Chem-Nuclear Systems, Columbia, SC, 1999 (available from NRC public document room)

2.3 Eco-Pak Specialty Packaging, Safety Analysis Report for the Model ESP-30X Protective Shipping Package for 30-Inch UF6 Cylinders, Revision 2, COC 71-9284, Eco-Pak Specialty Packaging, Division of the Columbiana Boiler Company, Columbiana, OH, 2000 (available from NRC public document room)

2.4 American National Standards Institute, Standard for Nuclear Materials-Uranium Hexaflouride-Packaging for Transport, ANSI N14.1, Washington, DC.

3.1 Johnson, P. E., and Michelhaugh, R. D., "Transportation Routing Analysis Geographic Information System (WebTRAGIS) User's Manual", ORNL/TM-2000/86, Oak Ridge National Laboratory. (2000)

3.2 Saricks, C. L., and Tompkins, M. M., "State-Level Accident Rates of Surface Freight Transportation: A Reexamination", ANL/ESD/TM-150, Argonne National Laboratory. (1999)

4.1 U.S. Dept. of Commerce (NOAA), and U.S. Dept. of Energy (NREL), "Solar and Meteorological Surface Observation Network, 1961-1990", CD-ROM, Ver. 1. (1993)

6.1 Ammerman, D. J., "A Method for Relating Impacts with Yielding and Unyielding Targets", Proceedings of the High Level Waste Management Conference, Tucson, AZ. (1992)

6.2 Ammerman, D. J., "A Method for Comparing Impacts with Real Targets to Impacts onto the IAEA Unyielding Target", Proceedings of PATRAM 92, Yokohama, Japan. (1992)

6.3 Taylor, L. M. and Flanagan, D. P., "PRONTO-3D: A Three Dimensional Transient Solid Dynamics Program", SAND87-1912, Sandia National Laboratories, Albuquerque, NM. (1987)

6.4 Gonzales, A., “Target Effects on Package Response: An Experimental and Analytical Evaluation”, SAND86-2275, Sandia National Laboratories, Albuquerque, NM. (1987)

6.5 Bonzon, L. L., “Final Report on Special Impact Tests of Plutonium Shipping Containers: Description of Test Results”, SAND76-0437, Sandia National Laboratories, Albuquerque, NM. (1977)

6.6 Waddoups, I. G., “Air Drop Test of Shielded Radioactive Material Containers”, SAND75-0276, Sandia National Laboratories, Albuquerque, NM. (1975)

6.7 Young, E. M., “SST-2/90 Scale Model Impact Tests Test Report,” Sandia National Laboratories, Albuquerque, NM (UCNI). (1995)

7.1 MSC PATRAN/Thermal Version 2001, Release 2, MSC.Software Corporation, Santa Ana, California, http://www.mscsoftware.com .

Distribution

1 MS0701 P.B. Davies, 6100

1 MS0718 K.B. Sorenson, 6141

1 MS0718 D.J. Ammerman, 6141

1 MS0718 C. Lopez, 6141

1 MS0405 J.S. Ludwigsen, 12333

5 MS0718 G.S. Mills, 6141

1 MS0718 R.F. Weiner, 6141

1 MS9018 Central Technical Files, 8945-1

2 MS0899 Technical Library, 9616

1 MS0612 Review & Approval Desk, 9612
For DOE/OSTI

1 U.S. Dept. of Energy
National Transportation Program Office
Attn.: S.C. Hamp
P.O. Box 5400
Albuquerque, NM 87185

1 U.S. Nuclear Regulatory Commission
Attn.: A. Giantelli
MS O13-D13
Washington, DC 20555-0001